Allelic barley MLA immune receptors recognize sequence-unrelated avirulence effectors of the powdery mildew pathogen

Xunli Lu[a,1], Barbara Kracher[a,1], Isabel M. L. Saur[a], Saskia Bauer[a], Simon R. Ellwood[b], Roger Wise[c,d], Takashi Yaeno[e], Takaki Maekawa[a,2], and Paul Schulze-Lefert[a,2]

[a]Department of Plant-Microbe Interactions, Max Planck Institute for Plant Breeding Research, Cologne D-50829, Germany; [b]Centre for Crop and Disease Management, Department of Environment and Agriculture, Curtin University, Bentley, Perth, WA 6102, Australia; [c]Corn Insects and Crop Genetics Research, Agricultural Research Service, US Department of Agriculture, Ames, IA 50011-1020; [d]Department of Plant Pathology and Microbiology, Center for Plant Responses to Environmental Stresses, Iowa State University, Ames, IA 50011-1020; and [e]Faculty of Agriculture, Ehime University, Matsuyama, Ehime 790-8566, Japan

Contributed by Paul Schulze-Lefert, August 4, 2016 (sent for review June 20, 2016; reviewed by Sophien Kamoun, Beat Keller, and Brian J. Staskawicz)

Disease-resistance genes encoding intracellular nucleotide-binding domain and leucine-rich repeat proteins (NLRs) are key components of the plant innate immune system and typically detect the presence of isolate-specific avirulence (AVR) effectors from pathogens. *NLR* genes define the fastest-evolving gene family of flowering plants and are often arranged in gene clusters containing multiple paralogs, contributing to copy number and allele-specific *NLR* variation within a host species. Barley *mildew resistance locus a* (*Mla*) has been subject to extensive functional diversification, resulting in allelic resistance specificities each recognizing a cognate, but largely unidentified, AVR_a gene of the powdery mildew fungus, *Blumeria graminis* f. sp. *hordei* (*Bgh*). We applied a transcriptome-wide association study among 17 *Bgh* isolates containing different AVR_a genes and identified AVR_{a1} and AVR_{a13}, encoding candidate-secreted effectors recognized by *Mla1* and *Mla13* alleles, respectively. Transient expression of the effector genes in barley leaves or protoplasts was sufficient to trigger *Mla1* or *Mla13* allele-specific cell death, a hallmark of NLR receptor-mediated immunity. AVR_{a1} and AVR_{a13} are phylogenetically unrelated, demonstrating that certain allelic MLA receptors evolved to recognize sequence-unrelated effectors. They are ancient effectors because corresponding loci are present in wheat powdery mildew. AVR_{A1} recognition by barley MLA1 is retained in transgenic *Arabidopsis*, indicating that AVR_{A1} directly binds MLA1 or that its recognition involves an evolutionarily conserved host target of AVR_{A1}. Furthermore, analysis of transcriptome-wide sequence variation among the *Bgh* isolates provides evidence for *Bgh* population structure that is partially linked to geographic isolation.

avirulence effectors | association analysis | R genes | plant-microbe interactions | powdery mildew

Encounters between flowering plants and pathogenic microbes often trigger host innate immune responses that are initiated by cell-surface or intracellular immune receptors upon the detection of pathogen-derived molecules (1). The latter are represented by the family of intracellular nucleotide-binding domain and leucine-rich repeat proteins (NLRs) that detect either the action or the structure of pathogen effectors inside host cells (2, 3). An effector molecule recognized by an NLR-type disease resistance (R) protein is designated an avirulence (AVR) effector, and these effector variants are typically present only in particular isolates ("races") of a pathogen species.

R genes encoding NLR-type receptors are frequently members of larger gene families, organized in complex clusters of paralogous genes, and can evolve through tandem and segmental gene duplications, recombination, unequal crossing-over, point mutations, and diversifying selection (2, 4). There are several examples of allelic series of NLR-type *R* genes known in plants (5–10). In these cases, multiple distinct recognition specificities evolved in the host population at a single *R* gene with each allele detecting a corresponding strain-specific *AVR* in the pathogen population. Such multiallelic NLR-type *R* genes are particularly interesting for exploring mechanisms underlying the coevolution of host and pathogen—for example, whether the corresponding *AVR* effectors evolved by sequence variation in a single effector gene or gene family or by innovation of phylogenetically unrelated *AVRs* (11, 12).

The ascomycete powdery mildews infect ∼10,000 angiosperm species, including many crops (13). As obligate biotrophic pathogens, their growth and reproduction is entirely dependent on living host cells. Filamentous powdery mildews form morphologically complex structures during asexual pathogenesis and produce fruiting bodies (diploid cleistothecia) during sexual reproduction. After asexual reproduction, airborne haploid conidiospores germinate within minutes upon contact with plant aerial surfaces and penetrate the host epidermal cell wall. Subsequently, fungal germlings develop a specialized infection structure, called the haustorium, by invagination of the plant plasma membrane for nutrient uptake from host cells and presumed export of effectors. In temperate climes, a short time period (7–10 d) is sufficient for an asexual

Significance

Gene-for-gene immunity is frequently found in interactions between plants and host-adapted pathogens and reflects population-level diversification of immune receptors detecting matching pathogen effectors. We identified effector genes of a pathogenic powdery mildew fungus that are recognized by allelic variants of barley intracellular nucleotide-binding domain and leucine-rich repeat protein-type receptors. These pathogen effectors are phylogenetically unrelated, demonstrating that allelic immune receptors can evolve to recognize sequence-unrelated proteins. Conserved effector recognition in distantly related *Arabidopsis* indicates that the underlying mechanism is not restricted to monocotyledonous plants. Furthermore, our study reveals that the expression of a fungal avirulence effector alone is necessary and sufficient for allele-specific mildew resistance locus A receptor activation in planta.

Author contributions: X.L., T.M., and P.S.-L. designed research; X.L., I.M.L.S., S.B., and T.M. performed research; S.R.E., R.W., and T.Y. contributed new reagents/analytic tools; B.K. analyzed data; and X.L., B.K., T.M., and P.S.-L. wrote the paper.

Reviewers: S.K., The Sainsbury Laboratory; B.K., University of Zürich; and B.J.S., University of California Berkeley.

The authors declare no conflict of interest.

Freely available online through the PNAS open access option.

Data deposition: The sequences reported in this paper have been deposited in the Gene Expression Omnibus (GEO) database, www.ncbi.nlm.nih.gov/geo (accession no. GSE83237).

[1]X.L. and B.K. contributed equally to this work.

[2]To whom correspondence may be addressed. Email: schlef@mpipz.mpg.de or maekawa@mpipz.mpg.de.

This article contains supporting information online at www.pnas.org/lookup/suppl/doi:10.1073/pnas.1612947113/-/DCSupplemental.

reproduction cycle, and the nature of airborne conidiospores ensures an efficient infection and spread of the pathogen to neighboring plants (14).

Annotated draft genome sequences are available for three powdery mildew species, each belonging to a different tribe of the order *Erysiphales* (15). These genomes display genome-size expansion mainly due to massive retrotransposon proliferation, and the observed gene losses might reflect genomic adaptations to an exclusively biotrophic lifestyle (15). In the best-characterized genome, established from the DH14 strain of the barley powdery mildew *Blumeria graminis* f. sp. *hordei* (*Bgh*), it was shown that >7% of all annotated genes encode candidates for secreted effector proteins (CSEPs; ref. 16). This *Bgh* effector repertoire of 491 proteins was grouped into 72 families of up to 59 members. Subsequent genome comparisons among three *Bgh* isolates and four isolates of the wheat powdery mildew fungus *Blumeria graminis* f. sp. *tritici* (*Bgt*) revealed that the genome structure of both species is characterized by an isolate-specific mosaic of monomorphic and polymorphic DNA blocks (17, 18). These studies also showed that *Bgh* and *Bgt* became reproductively isolated 6.3 million (±1.1 million) years ago, which is after the divergence of the sister Triticeae species barley and wheat (8 million to 9 million years ago; ref. 19). Estimates of the divergence time of the alternating isolate-specific monomorphic and polymorphic regions in both *Bgh* and *Bgt* genomes are >5,000 y, implying that these genome mosaics are the product of rare outbreeding events (by sexual reproduction) followed by frequent asexual (clonal) reproduction, which maintains the haploid genome structure in the respective pathogen populations. However, details on the phylogenetic diversification within *Bgh* or *Bgt* populations are largely unknown because the number of isolates for which genome-wide information is available is too low.

Domesticated barley and wheat cultivars contain numerous powdery mildew *R* gene loci, dispersed through their genomes, which were introgressed by humans from their corresponding wild relatives (20). For unknown reasons, in both barley and wheat, one of these powdery mildew *R* genes, designated *Mla* and powdery mildew 3 (*Pm3*), has been subject to exceptional functional diversification, documented by large numbers of allelic *Mla* or *Pm3* recognition specificities (i.e., resistance alleles each detecting a matching *Bgh* or *Bgt* AVR effector). Interestingly, however, some wheat *Pm3* alleles confer overlapping, but distinct, resistance specificities (21). In addition, the *Mla* orthologs *Sr33* in wheat (22) and *Sr50* in rye (23) confer resistance to the devastating Ug99 stem rust pathogen *Puccinia graminis* f. sp. *tritici* (*Pgt*), even though *Pgt* and *Bgh* belong to Basidiomycota and Ascomycota phyla, respectively (22). Barley *Mla* and wheat *Pm3* both encode intracellular NLRs with an N-terminal coiled-coil (CC) domain, but lacking significant sequence relatedness (24), whereas the deduced protein sequences of 23 characterized barley *Mla* resistance alleles exhibit >90% sequence identity, and 17 known wheat *Pm3* resistance alleles share >97% sequence identity. Diversifying selection among resistance alleles of *Mla* and *Pm3* is largely confined to the C-terminal LRR region of the receptors (8, 9). Of note, barley *Mla1* confers race-specific disease resistance to a *Bgh* isolate carrying the cognate avirulence gene AVR_{a1} in transgenic *Arabidopsis thaliana*, suggesting ∼150 million years of evolutionary conservation in the underlying immune mechanism (25). Recently, the *Bgt* avirulence gene $AVR_{Pm3a2/f2}$, which is recognized by the *Pm3a* and *Pm3f* alleles and encodes a typical CSEP that belongs to an effector family of 24 members, was isolated (18, 26). In *Bgh*, genetic linkage analysis revealed both linked and unlinked AVR_a loci and AVR_{a10}, which is recognized by barley *Mla10*, was found to be a member of the *EKA* gene family that is derived from part of a class I-LINE retrotransposon (27–29). It is still unclear whether other *Mla* or *Pm3* resistance alleles detect sequence-related family members of *EKA* or $AVR_{Pm3a2/f2}$, respectively. Thus, the molecular basis of multiallelic functional diversification in barley *Mla* and wheat *Pm3* and the evolutionary history of matching powdery mildew effectors remain unresolved.

Owing to the predominant clonal propagation of powdery mildews, we hypothesized that a transcriptome-wide association study could identify AVR_a candidates among 17 *Bgh* isolates collected from four distant geographic regions. In parallel, AVR_a profiles of each isolate were determined with a collection of near-isogenic barley lines containing different *Mla* recognition specificities and then associated with isolate-specific sequence variation in the transcriptomes. This method identified AVR_{a1} and AVR_{a13}, both encoding CSEPs, recognized by *Mla1* and *Mla13* alleles, respectively. These two AVR_a genes are *Blumeria*-specific gene innovations and are phylogenetically unrelated. In addition, our study reveals evidence for a *Bgh* population structure that is in part linked to geographical isolation.

Results

Transcriptome-Wide Single Nucleotide Polymorphism Analysis Reveals Population Structure of *Bgh* Isolates. We performed a genetic association analysis between sequence polymorphisms and AVR_a-mediated avirulence phenotypes among 17 *Bgh* isolates collected from Europe, North America, Australia, and Japan (Fig. S1*A*). The avirulence profile of each fungal isolate was determined by using a panel of near-isogenic barley lines (NILs) of accession Manchuria carrying *Mla1*, *Mla6*, *Mla7*, *Mla10*, *Mla13*, or *Mla15* recognition specificities (30). Infection phenotypes were scored into five macroscopically distinguishable infection types (ITs) at 9 d after spore inoculation on detached barley leaves (Fig. S1*B* and Table S1). These ITs ranged from undetectable *Bgh* colony formation without and with patches of leaf cell death (IT1 and 2, respectively), restricted colony formation with underlying cell death patches (IT3) to unrestricted colony formation with or without leaf chlorosis (IT4 and 5, respectively) (9). When we rated ITs 1–3 as "avirulent interactions," the reference isolate DH14 (15) was found to contain AVR_a genes recognized by *Mla1*, *Mla6*, *Mla7*, *Mla13*, and *Mla15* (Table S1), consistent with an independent earlier AVR_a profiling of this isolate (28). When applying the same avirulence classification, the avirulence profiles of the *Bgh* isolates against *Mla7* and *Mla15* were identical, although there were minor, but reproducible, IT differences between these two NILs (Table S1). Sequencing of leaf-derived cDNA revealed the presence of *Mla7* transcripts in both NILs, although different donor barley lines were originally used for introgression of the *Mla7* and *Mla15* recognition specificities (30). The Manchuria NILs were generated >40 y ago with a set of *Bgh* isolates that differ from our strains and before the molecular isolation of *Mla* (24, 31–33). Thus, it is possible that the introgressed segment of the "*Mla15* NIL" harbors, besides *Mla7*, an additional powdery mildew *R* gene that confounded introgression of the correct *Mla* recognition specificity. We conclude that our classification system for AVR_a-dependent avirulence profiles among the 17 *Bgh* isolates is sufficiently robust against minor IT variation.

To extract the genetic polymorphisms among these *Bgh* isolates, we sequenced the transcriptomes of 16 isolates (except reference isolate DH14) at 16 and 48 h post conidiospore inoculation (hpi) and compared these with the published whole-genome sequence draft for DH14 (15). RNA sequencing of *Bgh*-infected barley leaf tissue resulted in 20 million to 170 million sequenced fragments/reads per sample (comprising both barley and *Bgh* RNA), of which between 0.5 million and 8 million reads could be uniquely (mapping quality ≥ 10) mapped onto the DH14 reference genome (Table S2). The subsequent single nucleotide polymorphism (SNP) calling identified between 8,000 and 90,000 high-quality SNPs for the individual isolates (Table S2). We also performed SNP calling on the combined alignment data from all of the isolates to extract a collective SNP set over all isolates for the transcriptome-wide association analysis. An initial population structure analysis on a set of high-quality synonymous SNPs identified a distinct Australian clade (Fig. 1 *A* and *B*), but otherwise no further geographic

patterns among the 17 isolates. A visualization of the SNP distribution along the 15 largest contigs of the DH14 draft genome, representing 2.1% of the genome, including all high-quality SNPs for each isolate further confirmed the unique SNP pattern for the Australian isolates (Fig. S2). Additionally, these analyses revealed that the Japanese isolate RACE1 (34) contains an exceptionally large number of SNPs and a unique genotype/SNP pattern compared with all other isolates (Fig. 1 *A* and *B*, Fig. S2, and Table S2). Because this highly divergent genotype could confound genetic association tests among the remaining 16 isolates, we excluded RACE1 from the association test.

Genetic Association Analysis Identifies Candidate AVR_a Genes. We obtained a set of 67,385 high-confidence SNPs from the sequenced 15 isolates and DH14 (excluding RACE1 SNPs) with an alternate allele frequency of at least 10% in the combined alignment data. We further extracted the 6,982 diallelic SNPs that are predicted to introduce nonsynonymous substitutions in the DH14 reference proteins and tested each for their association with the observed avirulence profiles using Fisher's exact test (Fig. 1*C*). However, this analysis of individual variants is likely insufficient to detect all candidates because a virulence phenotype might be caused by different nonsynonymous SNPs in the same gene of virulent isolates. Thus, we additionally integrated the high-confidence nonsynonymous SNPs over each gene and also tested these genewise collapsed variants for association with the observed avirulence profiles using Fisher's exact test (Fig. 1*D*).

Based on the latter genewise collapsed variants, we identified *bgh00029* as the top ranking candidate for AVR_{a1} ($P = 0.011$) (Fig. 1*D*). Moreover, the two individual SNPs in this gene also ranked among the top five of the individual variants, according to the observed Fisher test P values ($P = 0.011$ for both) (Fig. 1*C*), providing further support for this candidate. *bgh00029* encodes a 118-amino acid protein with a predicted signal peptide at position 1–26 (Fig. 2 *A* and *B* and Fig. S3*A*) and represents one of the previously annotated CSEPs, designated CSEP0008, which was previously found to show weak structural similarity to ribonucleases (16). In almost all of the isolates, this gene was highly expressed at both 16 and 48 hpi (Dataset S1A), but in one of the virulent isolates, NCI, the respective transcripts were undetectable (Fig. 2*A*). The deduced proteins from the virulent isolates, CC88 and A6, carry the same two amino acid substitutions, P32R and V74A (Fig. 2*B* and Fig. S3*A*). We also examined the corresponding transcript sequence of isolate RACE1, which is virulent on *Mla1* containing barley (Table S1). This isolate contains multiple nonsynonymous SNPs in the *bgh00029* transcript, which interfered with read-mapping at the respective region (Fig. 2*A*) and led to four amino acid substitutions adjacent to the signal peptide: R27Q, Q30H, P32K, and L37I. Notably, one amino acid substitution from proline to a positively charged amino acid (Arg or Lys) occurred at position 32 in all three virulent isolates (RACE1, CC88, and A6; Fig. 2*B*), suggesting that it might be important for the avirulence activity. For simplicity, hereafter the deduced proteins encoded at the *bgh00029* (*CSEP0008*) locus in the avirulent isolates are named AVR_{A1}; those in the virulent isolates CC88 and A6 are designated AVR_{A1}-V1; and the protein variant in RACE1 is termed AVR_{A1}-V2 (Fig. 2*B*).

Unlike for AVR_{a1}, the association test for AVR_{a13} yielded only candidates without a clear secretion signal. Because a *CSEP* gene was identified as a candidate for AVR_{a1}, we manually inspected genotype and expression patterns of the powdery mildew CSEP transcripts using the Integrative Genomics Viewer (IGV) (35, 36) to examine whether any highly expressed *CSEP* genes were associated with the observed avirulence phenotypes. We noticed that at the *bghG002861000001001* (*CSEP0372*) locus, one of the two virulent isolates, CC52, carries a nonsynonymous substitution, whereas no sequencing reads were mapped to the 3′ region of the coding sequence of this gene in the other virulent isolate, B103 (Fig. 2*C*).

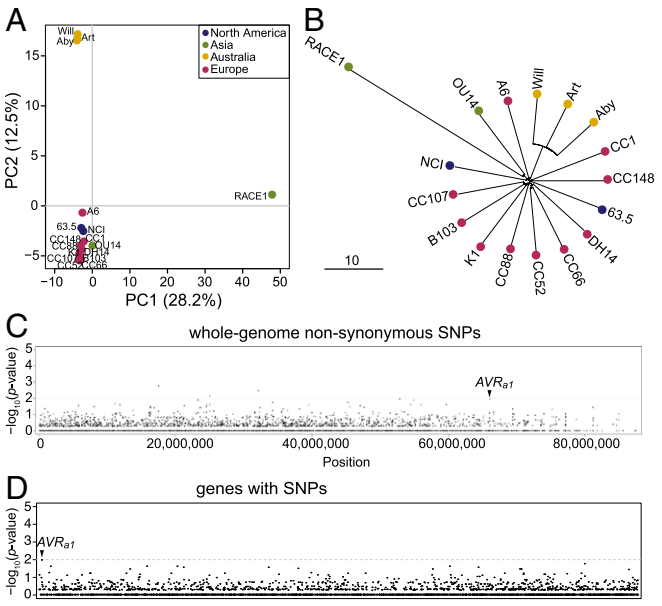

Fig. 1. Population structure of *Bgh* isolates and association test results for AVR_{a1}. (*A*) PCA of 17 *Bgh* isolates based on 5,049 high-quality synonymous SNPs separates RACE1 (PC1) and the Australian isolates (PC2), whereas all other isolates clustered together irrespective of their geographic origin. (*B*) Neighbor-joining (NJ) tree based on the same 5,049 high-quality synonymous SNPs (2,081 of which are specific to RACE1). (*C*) Manhattan plot summarizing the individual SNP association results for AVR_{a1}. The *x* axis represents all contigs of at least 1 kb in the *Bgh* DH14 genome, sorted by decreasing contig length; the *y* axis shows $-\log_{10} P$ values for all coding SNPs with predicted effect on the amino acid sequence. The position of the two subsequently verified candidate SNPs is marked in the plot with an arrowhead. (*D*) Manhattan plot summarizing the genewise association results for AVR_{a1}. The *x* axis represents the *Bgh* DH14 genes, sorted by *Bgh* gene ID; the *y* axis shows $-\log_{10} P$ values for all genes with at least one nonsynonymous coding SNP. The subsequently verified candidate AVR_{a1} gene is marked in the plot with an arrowhead.

Because our bioinformatics pipeline was designed for the analysis of SNP data, this gap in the read alignment for isolate B103 escaped our association screening.

CSEP0372 encodes a 122-amino acid protein with a predicted signal peptide at positions 1–21 (Fig. 2*D*), which shows strong structural homology to ribonucleases based on several protein structure prediction tools (37–39). The corresponding protein from the virulent isolate CC52 is predicted to carry a premature stop codon at position 81 (Fig. 2*D* and Fig. S3*B*). Because the respective locus in the isolate B103 expressed a poly-A-tailed mRNA, we obtained the actual transcript sequence in this isolate by 3′-rapid amplification of cDNA ends (3′-RACE) and investigated the cause for the lack of mapped reads in the 3′ region of the gene. We found a 326-bp DNA insertion at the 3′ end of *CSEP0372* transcript in this isolate (Fig. S3 *B* and *C*), which accounted for the loss of read mapping in this gene region (Fig. 2*D*). Similar DNA sequences are frequently found in the DH14 genome (>230 contigs). Because of the insertion, eight C-terminal amino acids of the corresponding protein are replaced by five unrelated amino acids (Val-Arg-Ala-Thr-Leu) after position 115 (Fig. 2*D* and Fig. S3 *B* and *C*). Nonsynonymous SNPs were not only found in the virulent isolates, but also in the avirulent isolates CC107 and RACE1 in this gene. The isolate CC107 carries one SNP substituting Arg to a similar type of amino acid, Lys at position 117, whereas the isolate RACE1 carries three nonsynonymous SNPs, which cause the three substitutions H45Y, H59Y, and R117K (Fig. 1*E*). Hereafter, the proteins encoded at the *bghG002861000001001* (*CSEP0372*) locus in the avirulent isolates DH14, CC107, and

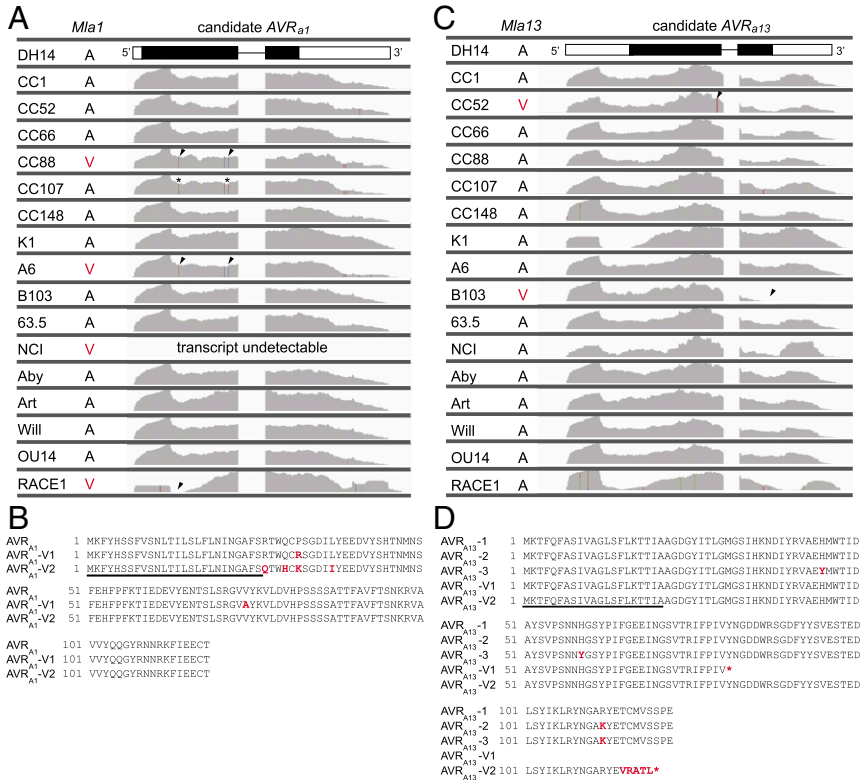

Fig. 2. Association of transcript polymorphisms with avirulent phenotypes of *Bgh* isolates. (*A*) Visualization of the identified AVR_{a1} candidate locus, indicating on the left the response of the barley Manchuria *Mla1* NIL (30) against each *Bgh* isolate. A, avirulent; V, virulent. (*B*) AVR_{A1} protein sequence with the predicted signal peptide indicated by a black line. The amino acid substitutions in the two identified virulent protein versions AVR_{A1}-V1 and -V2 are highlighted in red. (*C*) Visualization of the identified AVR_{a13} candidate locus, indicating on the left the response of the barley Manchuria *Mla13* NIL against each *Bgh* isolate. (*D*) AVR_{A13} protein sequence with the predicted signal peptide indicated by a black line. The corresponding amino-acid substitutions in AVR_{A13}-2, -3, -V1, and -V2 compared to AVR_{A13}-1 are highlighted in red. In *A* and *C*, for isolate DH14 (reference genome), the corresponding gene structure for AVR_{a1} (*A*) or AVR_{a13} (*C*) is shown with UTRs (white boxes), coding sequence (black boxes), and introns (black line). For all other isolates, RNA-seq coverage and all observed SNPs relative to DH14 (marked as colored bars, where each color represents one nucleotide with red, T; green, A; blue, C; and brown, G) were visualized by using the Integrative Genomics Viewer. The locations of the different virulence-inducing changes found in each of the virulent isolates are marked with arrowheads. The asterisks mark two positions in *Bgh* isolate CC107, where half of the RNA-seq reads from this isolate carried the avirulent (reference) allele and half carried the virulent (alternate) allele.

RACE1 are designated AVR_{A13}-1, AVR_{A13}-2, and AVR_{A13}-3, respectively, and those in the virulent isolates CC52 and B103 are termed AVR_{A13}-V1 and AVR_{A13}-V2 (Fig. 2*D*), respectively. Our computational pipeline failed to identify AVR_{a6} and AVR_{a7} candidates, and we were unable to reidentify AVR_{a10} (27–29).

Transient Expression of AVR_{a1} and AVR_{a13} in Barley Leaves Triggers Cell Death in Genotypes Carrying *Mla1* and *Mla13* Recognition Specificities, Respectively. To determine whether the identified AVR_{a1} and AVR_{a13} candidates have avirulence activity, we examined whether transient expression of the fungal genes triggered specific responses in barley lines containing matching *Mla* recognition specificities. For each candidate, appropriate expression constructs without the signal peptide sequence were generated in the pIPKb002 overexpression vector that harbors a maize ubiquitin promoter for transgene expression in cereals (40). The resulting expression constructs were delivered into second leaves of a series of Manchuria NILs by infiltration of the *Agrobacterium tumefaciens* strain AGL1 on the adaxial side of leaves. At 9–14 d after infiltration of *Agrobacteria* harboring the expression construct for AVR_{a1}, intense brown spots or blotches (suggestive of a host cell death response) appeared on the leaves of the NIL expressing *Mla1*, but not on leaves of NILs expressing *Mla13* or *Mla6*, and were also undetectable on the Manchuria recurrent parent line lacking a known *Mla* recognition specificity (Fig. 3*A*). In addition, no responses were detected upon the delivery of the expression construct of AVR_{a1}-*V1* or AVR_{a1}-*V2* in the leaves of the *Mla1* NIL (Fig. 3*A*). Clear brown spots were detected upon the delivery of the expression constructs for AVR_{a13}-*1* or AVR_{a13}-*3* in the leaves of the *Mla13* NIL at 5–9 d after infiltration (Fig. 3*B*), whereas these were undetectable on leaves of *Mla1* or *Mla15* NILs or on leaves of the Manchuria recurrent parent (Fig. 3*B*). Furthermore, no responses were detected upon the delivery of the expression constructs for AVR_{a13}-*V1* or AVR_{a13}-*V2* in leaves of the *Mla13* NIL (Fig. 3*B*). Together, these data suggest that *Mla1* and *Mla13* specifically recognize AVR_{a1} and AVR_{a13}, respectively.

To further validate the avirulence activity of AVR_{a1} and AVR_{a13}, we used a protoplast system to examine barley leaf cell viability upon delivery of the respective AVR_a constructs into host cells containing different *Mla* recognition specificities. The protoplast system has been used as a sensitive tool to study functions of various avirulence proteins in *Arabidopsis* (41, 42), tomato (43), and rice (44). An expression construct for the firefly luciferase gene under a maize ubiquitin promoter was used as a reporter, and the luciferase activity was quantified as proxy for cell viability. We tested protoplasts derived from a stable transgenic barley line expressing *Mla1* under its native 5′-regulatory sequences, which was generated in cultivar Golden Promise (45). As negative controls, we used nontransgenic Golden Promise and a transgenic barley line expressing *Mla6* under its native 5′-regulatory sequences generated in the same genetic background (45). We detected a

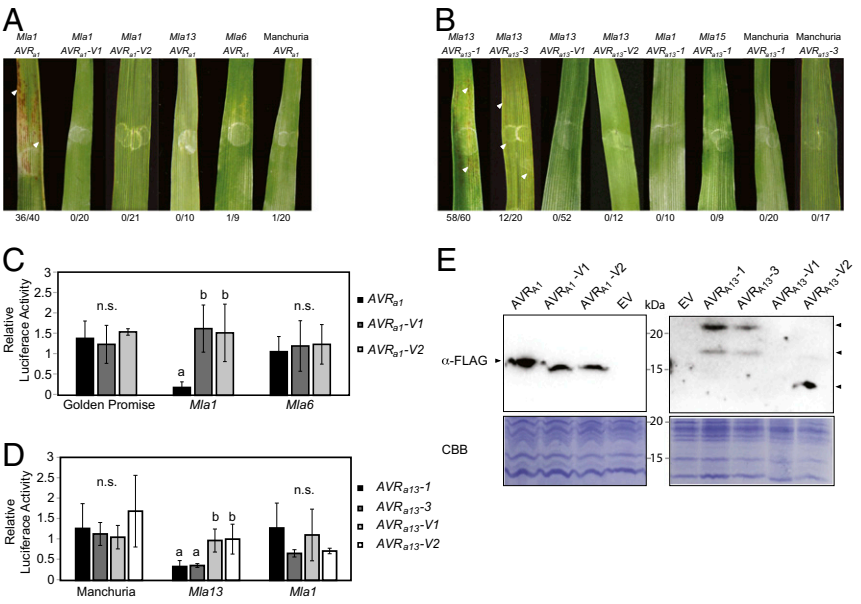

Fig. 3. Transient expression of AVR_{a1} and AVR_{a13} in barley triggers cell death in genotypes carrying corresponding *Mla* recognition specificities. (*A* and *B*) Expression cassettes for AVR_{a1}, AVR_{a1}-*V1*, and *V2* (*A*) or AVR_{a13}-*1*, *-3*, *-V1*, and *-V2* (*B*) without signal peptides were delivered into barley leaves by *Agrobacterium* infiltration. (*A*) Expression of AVR_{a1}, but not AVR_{a1}-*V1* or *-V2*, induces a specific cell death response in an *Mla1* NIL (30), but not in *Mla13* and *Mla6* NILs or Manchuria. (*B*) Expression of AVR_{a13}-*1* and *-3*, but not AVR_{a13}-*V1* or *-V2*, induces a specific cell death response in a *Mla13* NIL, but not in *Mla1* and *Mla15* NILs or Manchuria. White arrows indicate necrotic leaf patches. Incidence of infiltrated leaves with cell death response is indicated for each genotype. (*C* and *D*) Relative luciferase activity after transformation of AVR_{a1}, AVR_{a1}-*V1*, and *-V2* into barley protoplasts generated from Golden Promise without or with *Mla1* or *Mla6* transgenes (*C*) or transformation of AVR_{a13}-*1*, *-3*, *-V1*, and *-V2* into barley protoplasts generated from Manchuria, *M1a13*, or *Mla1* NILs (*D*). Luciferase activity was normalized for each plant line by setting the detected luminescence for the corresponding empty vector transfection to 1. For each plant genotype, differences between samples were assessed by using analysis of variance (ANOVA) and subsequent Tukey post hoc tests. Observed ANOVA *P* values were as follows: Golden promise: $P = 0.51$, *Mla1*: $P = 6.7e\text{-}07$, and *Mla6*: $P = 0.77$ (*C*); Manchuria: $P = 0.40$, *Mla13*: $P = 4.4e\text{-}05$, and *Mla1*: $P = 0.27$ (*D*). Samples marked by identical letters in the plot did not differ significantly ($P < 0.05$) in the Tukey test for the corresponding genotype. n.s., not significant. (*E*) Steady-state levels of the epitope-tagged AVR_{A1} and AVR_{A13} variants in barley protoplasts. FLAG-tagged effector constructs were delivered into protoplasts of Golden Promise for AVR_{A1}, AVR_{A1}-V1, and -V2 expression or Manchuria for AVR_{A13}-1, -3, -V1, and -V2 expression. Protoplasts were collected 18 h after transfection for Western blotting. Specific signals for the FLAG-tagged proteins are indicated by arrowheads.

significant reduction of luciferase activity in a *Mla1*-AVR_{a1}–specific manner (Fig. 3*C*). Similarly, a significant reduction of luciferase activity was detected in an *Mla13*-AVR_{a13}–specific manner in the Manchuria background (Fig. 3*D*). Together, the recognition of AVR_{a1} and AVR_{a13} by the cognate *Mla* receptors resulted in an effector-triggered cell death response.

We generated additional expression constructs for epitope-tagged AVR_{A1}, AVR_{A13}, and their variants found in our *Bgh* collection to examine the steady-state level of these proteins in barley protoplasts. Because the four N-terminal amino acid substitutions in AVR_{A1}-V2 of isolate RACE1 escape recognition by MLA1 (Fig. 2*B*), the N-terminal region of AVR_{A1} might be particularly important for its recognition. Therefore, a single FLAG-tag was fused to the C termini of AVR_{A1}, AVR_{A1}-V1, and -V2. Because the C-terminal residues seem to be important for MLA13-mediated recognition of AVR_{A13} (Fig. 2*D*), a single FLAG-tag was fused to the N termini of AVR_{A13}-1, -3, -V1, and -V2. The C-terminally tagged AVR_{A1} and the N-terminally tagged AVR_{A13} variants were still specifically recognized by MLA1 and MLA13 in barley leaves and the protoplast system, despite few measurement outliers (Fig. S4). The epitope-tagged AVR_{A1}, AVR_{A1}-V1, and -V2 proteins were detected by Western blotting (Fig. 3*E*), suggesting that the loss of avirulence for AVR_{A1}-V1 and -V2 is not because of protein instability. Although epitope-tagged AVR_{A13}-1 and -3 were clearly detectable in protoplasts, AVR_{A13}-V1 was undetectable, and AVR_{A13}-V2 protein migrated faster (Fig. 3*E*), suggesting that loss of avirulence activity for AVR_{A13}-V1 and -V2 might be due to protein instability in planta.

AVR_{A1} Is Recognized by Barley MLA1 in Stable Transgenic *Arabidopsis* Plants. Barley *Mla1* confers *Bgh* isolate-specific resistance in *A. thaliana* (25). To examine whether AVR_{A1} expression is sufficient for recognition by barley MLA1 in dicotyledonous *A. thaliana*, we generated a series of transgenic *A. thaliana* plants in Col-0 expressing AVR_{A1} or one of the virulent variants, AVR_{A1}-V1, without signal peptide under control of the *A. thaliana ubiquitin* promoter. The expression constructs were designed to express either their native forms (i.e., without epitope tag) or C-terminally FLAG-tagged fusion proteins. The latter fusion protein retained the avirulence activity of AVR_{A1} in barley (Fig. S4 *A* and *C*). We selected T_1 lines based on transcript level of AVR_{a1} or steady-state level of the fusion proteins (Fig. S5 *A* and *B*). These T_1 lines were crossed with the previously established transgenic *A. thaliana* plants homozygous for the *Mla1* transgene in accession Col-0 (25) (Fig. 4 and Fig. S5).

The F_1 plants carrying *Mla1* and either AVR_{a1} or AVR_{a1}–*FLAG* died shortly after germination (63%) or showed severe growth retardation (37%) compared with their sister plants lacking AVR_{a1} and AVR_{a1}-*FLAG* (Fig. 4 *A* and *B* and Fig. S5 *C* and *D*). Importantly, wild-type–like growth was observed in plants carrying *Mla1*, irrespective of the presence or absence of AVR_{a1}-*V1–FLAG* (Fig. 4*C* and Fig. S5*E*). The AVR_{a1}-induced seedling lethality and plant growth retardation were dependent on the *Mla1* transgene, because it was not observed in the F_1 progeny of the transgenic plant carrying AVR_{a1} crossed with Col-0 (Fig. 4*D*). Together, these data provide evidence for specific recognition of AVR_{A1} by MLA1 in transgenic plants and exclude the possibility that additional *Bgh*-derived molecules other than

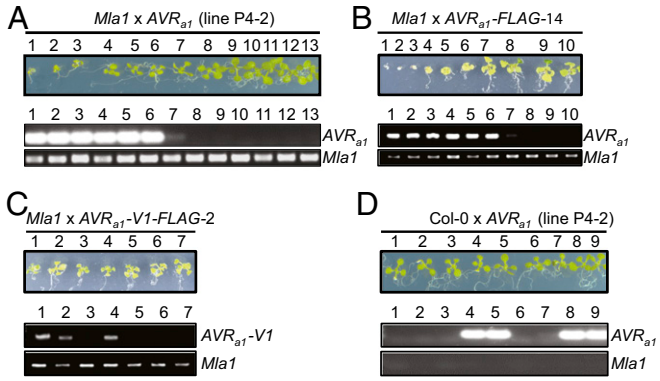

Fig. 4. AVR_{A1} is recognized by barley MLA1 in stable transgenic *Arabidopsis* plants. (*A*–*C*) Seedling growth of the F_1 progenies from crosses between homozygous *A. thaliana* transgenic plants carrying *Mla1* (25) and T_1 plants carrying constructs for expression of AVR_{a1} (*A*), AVR_{a1}-*FLAG* (*B*), or AVR_{a1}-*V1-FLAG* (*C*). (*D*) Col-0 plants were also crossed with AVR_{a1}. Plants carrying the *Mla1* transgene or Col-0 were used as the female parents. F_1 progenies were ordered by size when possible. Seedlings were grown on solid 1/2 MS medium for 14–16 d before the examination of seedling growth. The corresponding segregation patterns of the transgenes are shown in the lower panels.

AVR_{A1} are needed for effector recognition and immune receptor-mediated signaling in dicotyledonous *A. thaliana* (25).

AVR_{A1} and AVR_{A13} Are Sequence-Unrelated Ancient Effectors. The genome of *Bgh* isolate DH14 was previously predicted to harbor 491 *CSEP* genes, 402 of which were found to be grouped into 72 families based on their deduced full-length amino acid sequences (16). The entire set of *Bgh CSEP*s can be subdivided into two classes based on the protein size: one ranging from 100 to 150 amino acids and the other from 300 to 400 amino acids (16), with AVR_{A1} (118 aa) and AVR_{A13} (123 aa) belonging to the former class. Based on a Markov cluster (MCL) analysis of the 491 *Bgh* CSEPs, AVR_{A1} does not belong to a defined *CSEP* family, whereas AVR_{A13} represents one of three members of *CSEP* family 34 (16). AVR_{a13} is highly expressed at 16 and 48 hpi, whereas expression of the other two family members, *CSEP0371* and *CSEP0374*, was rarely detected at these time points (Dataset S1A), suggesting that AVR_{A13} plays an important role at the early invasive stage of powdery mildew infection.

To investigate the evolutionary history of AVR_{a1} and AVR_{a13}, we examined whether orthologous genes are present in the closely related wheat powdery mildew fungus, *Bgt*. It was reported that the genome of the reference *Bgt* isolate 96224 contains 472 *CSEP* genes (18). To search for *Bgt* orthologs of *Bgh* AVR_{a1} and AVR_{a13} and identify CSEP families across *formae specialis*, we performed an OrthoMCL (46) analysis on the combined *Bgh* and *Bgt* CSEP sets. Because AVR_{A1} and AVR_{A13}, lacking their signal peptides, were both sufficient to induce cell death responses in barley expressing cognate MLA receptors (Figs. 2–4), we used the protein sequences of both *Bgh* and *Bgt* CSEPs without signal peptides for OrthoMCL clustering. This method identified a total of 298 CSEP families, 193 of which represent single-copy orthologous gene pairs from each species (Dataset S1*B*). One of these 193 gene pairs consists of AVR_{A1} and its *Bgt* ortholog, BgtE-5560 (Fig. 5*A*). AVR_{A13} is grouped together with *Bgh* CSEP0371 and *Bgh* CSEP0374, as shown in a previous study (16). This CSEP family contains one *Bgt* CSEP, BgtE-5665, which is an ortholog of *Bgh* CSEP0374 (Fig. 5*B*). We also found corresponding genomic loci for BgtE-5560 and -5665 in the genomes of the other three sequenced *Bgt* isolates 94202, 70, and JIW2 (Fig. S6), indicative of their conservation across different *Bgt* isolates. Together, the presence of a family member from *Bgt* for both AVR_{a1} and AVR_{a13} suggests that common ancestors existed for both AVR_{a1} and AVR_{a13} before the reproductive isolation of *Bgh* and *Bgt*. In contrast, a previous study did not find homologous sequences of *CSEP0008* (AVR_{a1}) and *CSEP0372* (AVR_{a13}) in two other powdery mildew fungi, *Erysiphe pisi* and *Golovinomyces orontii* (16).

Discussion

Evidence for prevalent clonal over sexual *B. graminis* reproduction in natural environments, together with a short lifespan of its airborne asexual propagules—called conidiospores, whose survival declines rapidly within 24 h—predicts a limited geographic dispersal for clonal progeny (17, 18, 47). Although these *Bgh* features could explain a distinctive population lineage detected for the Australian isolates (Fig. 1 *A* and *B* and Fig. S2), our sample size is still too small to draw general conclusions. Nevertheless, the finding that both North American and one Japanese isolate, OU14, are not clearly separated from the 10 European samples (Fig. 1 *A* and *B* and Fig. S2) indicates a potential long-distance dispersal of these three strains, perhaps via long-lived cleistothecia on plant litter linked to human migration or barley domestication. Consistent with this idea is that isolate OU14 has been recently collected in Japan in 2014 from a barley cultivar, Haruna Nijo, derived from a cross between European accessions and Japanese landraces (48). In contrast, the highly divergent RACE1 was a dominant Japanese *Bgh* race collected in the early 1950s on indigenous Japanese barley varieties that differ from the cultivars of European origin (34, 49). Despite an unclear separation of OU14 from the European isolates in the principal component analysis (PCA) (Fig. 1*A*), a neighbor-joining tree of all 17 strains indicates some relatedness to the other Japanese isolate, RACE1 (Fig. 1*B*). Thus, OU14 might be a progeny of a cross between Europe-derived and indigenous Japanese *Bgh* strains, possibly representing a genomic adaptation to the prevailing Japanese barley Haruna Nijo containing European and Japanese barley germplasm. In line with this assumption, visualization of the SNP distribution on the 15 largest DH14 contigs suggests that the OU14 genome contains some regions where the sequence is highly similar to those of European isolates (low SNP density), whereas other regions seem to be more divergent and might represent the contribution of Japanese races (Fig. S2). Because our present study is based on transcriptomic data and thus does not capture the intergenic regions, a detailed analysis of the genome structure is not feasible. Nevertheless, the distribution of

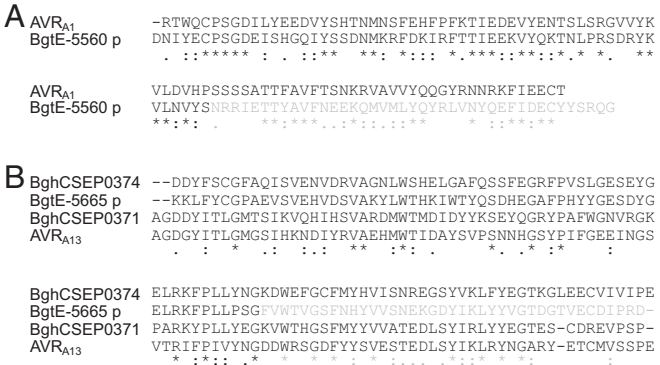

Fig. 5. Protein sequence alignment of AVR_{A1} and AVR_{A13} families. Protein sequences of the *Bgh* and *Bgt* members of the AVR_{A1} (*A*) and AVR_{A13} (*B*) CSEP families were aligned based on the protein annotations of the reference genomes of isolates DH14 (*Bgh*) and 96224 (*Bgt*), excluding the signal peptides. In black is the protein sequence representing the published annotations. In gray is the sequence of extended protein C termini for the respective *Bgt* proteins as predicted from the *Bgt* genome sequence (a corresponding nucleotide alignment is shown in Fig. S6), which was not included in the published annotation.

transcriptomic SNPs for the 17 isolates is in good agreement with the previously identified mosaic structure of *Bgh* genomes (17). Notably, some of the monomorphic regions between DH14, A6, and K1 (17) seem to be conserved among all isolates except RACE1 (Fig. S2, region I) or at least more generally conserved among the European isolates (Fig. S2, region II).

We have shown that association genetics can serve as an alternative for map-based isolation of powdery mildew AVR_a genes with genome-wide transcript information from as few as 16 *Bgh* isolates (excluding RACE1). However, the effector genotypes associated with the observed avirulence and virulence patterns were not only found to be SNPs in the *AVRa* genes, but also structural polymorphisms, including a DNA insertion in AVR_{a13} or complete absence of gene transcripts in one isolate for AVR_{a1}, which might result from a deletion of this gene or gene silencing (Fig. 2 *A* and *C*). Similarly, in a recent survey of an *AVR* locus comprising 108 *Magnaporthe oryzae* isolates, 81% of *AvrPib* polymorphisms leading to loss of avirulence resulted from TEs, whereas loss of avirulence due to SNPs was rare (0.6%; ref. 50). Thus, including information on SNPs, structural gene/transcript variants, and presence/absence of genes/transcripts in association studies is expected to significantly improve the identification of candidate *AVR* genes in eukaryotic filamentous pathogens.

In this work, we identified two *Bgh* avirulence genes, AVR_{a1} and AVR_{a13}, by association analysis between avirulence profiles and transcript polymorphisms among 17 *Bgh* isolates. Both identified avirulence genes encode CSEPs (16). AVR_{a1} and AVR_{a13} are sequence-unrelated, implying that they have been evolving independently from different ancestral genes, or, if they had a common ancestor, have been diverging rapidly. Additionally, we have shown that the predicted signal peptides of AVR_{A1} and AVR_{A13} are dispensable for specific recognition by MLA1 and MLA13, respectively (Fig. 3). This finding is consistent with the idea of a powdery mildew type II secretory-driven process in which the signal peptide becomes cleaved either during or after completion of effector translocation into the extracellular space between fungus and host (51). Intracellular localization of epitope-tagged MLA receptors in the cytoplasm and nucleus (45, 52) also implies subsequent uptake of the cleaved forms of AVR_{A1} and AVR_{A13} inside host cells and recognition by the immune sensors. Thus, it is likely that *Bgh* CSEPs are authentic effector molecules that act inside host cells.

Previous comparison of de novo annotated *Bgh* transcriptomes revealed evidence for conservation of their effector repertoire comprising 491 *CSEPs* (16, 17). Our work showed complete absence of AVR_{a1} transcripts or altered transcript structure leading to undetectable AVR_{A13}-V1 or the cleavage of AVR_{A13}-V2 proteins in planta, likely due to instability of these variants (Figs. 2*A* and 3*E*). These findings demonstrate that loss of individual and ancient *CSEP* genes, maintained for at least 6.3 million (±1.1 million) years, encoding AVR effectors, occurs in *Bgh* populations without apparent loss of pathogenicity, although the function of AVR_{a1} cannot be compensated by a sequence-related family member because this effector does not belong to one of the 72 CSEP families (16). It is possible that sequence-unrelated, but structurally and/or functionally similar, homologs encoded by other *Bgh* CSEPs might compensate for the loss of AVR_{a1} by interfering with the same host target(s). Alternatively, structurally unrelated CSEPs may interfere with different components belonging to the same host pathway targeted by AVR_{A1}, which is needed for virulence.

Barley *Mla* disease-resistance genes are subject to strong diversifying selection, as evidenced by >30 variants, each encoding a different resistance specificity that detects a corresponding *Bgh* AVR_a gene product (20). Among the 23 molecularly characterized MLA receptors, the C-terminal LRR domain is highly polymorphic (56% sequence identity), whereas the N-terminal CC domain is more conserved (87% sequence identity) (9). The polymorphic MLA LRR is critical for effector detection, as shown by a series of reciprocal domains swaps between MLA1 and MLA6, locating in each receptor a recognition domain for putative AVR effector proteins within different, but overlapping, LRR regions (53). One possibility is that functional diversification of allelic NLR variants is the result of a co-evolutionary process mediated by direct, iterative cycles of receptor and pathogen effector associations. This process is exemplified by direct interactions between allelic flax rust (*Melampsora lini*) effectors encoded at the *AVRL567* locus and allelic flax L NLRs L5 and L6, respectively (11, 54). However, hybridization of *AvrL567* probes to *M. lini* genomic DNA did not detect any related sequences, even at low stringency (55, 56). Therefore, *L* flax rust resistance alleles other than L5 and L6 likely detect sequence-unrelated *M. lini* effectors. A study on the allelic series of *RPP13* genes from *A. thaliana* revealed that only a single clade of *RPP13* alleles can recognize the allelic *ATR13* genes from *Hyaloperonospora arabidopsidis*, whereas an RPP13 protein from a different clade was found to recognize an unrelated *H. arabidopsidis* effector (12). Our findings contrast with those reported in rice for *Pik* NLR resistance alleles, each detecting matching allelic variants of *AVR-Pik* of the fungus *M. oryzae* by direct physical binding (10). Recognition of the sequence-unrelated AVR_{a1}, AVR_{a13} (Fig. 5), and the previously reported AVR_{a10} (28), by allelic *Mla1*, *Mla13*, and *Mla10* receptors, shows that additional mechanisms directing iterative cycles of receptor and pathogen effector adaptations can drive extensive functional diversification at a single *NLR* gene. Thus, it is possible that these three highly sequence-related MLA receptors (>91% sequence identity) might indirectly detect the presence of sequence-unrelated AVR_A effectors through modifications of a common effector target. In this scenario, individual AVR_A effectors are predicted to introduce distinctive protein modifications, either directly or indirectly to a shared host target. All MLA receptors would be expected to interact with this target, with each receptor sensing a different target surface or modification, mainly via the LRR domain. Recognition of AVR_{A1}, but not AVR_{A1}V-1, in transgenic *Arabidopsis* lines coexpressing barley MLA1 implies functional conservation of this common effector target between monocots and dicots. Because *Mla* orthologs in the closely related Triticeae species wheat and rye confer resistance to the wheat stem rust pathogen *Pgt* (22, 23), it is tempting to speculate that *Bgh* and *Pgt* effectors converge on the same effector target. Experimental evidence for convergence of effectors from unrelated pathogens on common host targets has been recently demonstrated in *A. thaliana* (55, 56). Similarly, it has been proposed that sequence-unrelated effectors form structurally similar proteins in the Ascomycete *Magnaporthe* and two Oomycete pathogens (57–59). Based on these examples, it is also possible that sequence-unrelated AVR_A effectors are structural homologs that are sensed by the LRR domain via direct binding.

The identification of two sequence-unrelated AVR effectors recognized by allelic immune receptors enables future experiments on the underlying recognition mechanism. The presented transcriptome-wide association study will spur the identification of additional *Bgh* AVR_A effectors, which will be important for reconstructing how allelic immune receptors have evolved in response to sequence-unrelated AVR effectors.

Materials and Methods

Plant Materials and Growth Conditions. The barley (*Hordeum vulgare* L.) cultivar (cv.) Manchuria (CI 2330) and Manchuria near isogenic lines, carrying *Mla1* (CI 16137), *Mla6* (CI 16151), *Mla7* (CI 16147), *Mla10* (CI 16149), *Mla13* (CI 16155), or *Mla15* (CI 16153) were described in ref. 30. Barley transgenic *Mla1-HA* (6E) and *Mla6-HA* (9E) plants were previously generated in the genetic background of barley cv. Golden Promise (45). Barley plants were grown at 19 °C, 70% relative humidity, and under a 16-h photoperiod. *A. thaliana* Col-0 plants were used to generate transgenic AVR_{a1} plants by

using Agrobacterium-mediated transformation using the floral dip method (60). The *Arabidopsis* stable transgenic line expressing *Mla1-HA* (47-2 in Col-0 background) was described (25). *Arabidopsis* plants were grown at 22 °C, 70% relative humidity, and under a 12-h photoperiod.

Fungal Isolates and Maintenance. *Bgh* isolate OU14 (Okayama University 14) was collected in 2014 from a barley cultivar, Haruna Nijo, grown at a nursery of the Institute of Plant Science and Resources, Okayama University (Okayama, Japan). Aby-00 was collected in September 2012 in Kojonup, Western Australia (GPS coordinates −34.0545, 117.2931). Art-001 was collected in April 2013 in Arthur River, Western Australia (GPS coordinates −33.3391, 117.0975). Will-005 was collected in September 2014 in Williams, Western Australia (GPS coordinates −33.0089, 116.9341) from a barley cultivar, Bass. The seven UK isolates (DH14, CC1, CC52, CC66, CC88, CC107, and CC148), the Danish isolate (B103), the two US isolates (63.5 and NCI), one of the Japanese isolates (RACE1), the German isolate (K1), and the Swedish isolate (A6) have been described (32, 34, 61–67). All isolates were maintained by inoculating conidiospores on a weekly basis onto 9-d-old detached first leaves placed on closed agar plates containing 1 mM benzimidazole. All isolates except RACE1 were maintained on leaves of barley cv. Ingrid that carries *Mla8*, whereas isolate RACE1 was maintained on barley cv. Manchuria.

RNA Extraction, RNA-Sequencing Analysis and SNP Calling. At 16 and 48 h after *Bgh* conidiospore inoculation, barley leaves or leaf-epidermal peels from susceptible cultivars were harvested to extract total RNA by using the RNeasy plant mini kit (Qiagen). RNA-sequencing (RNA-seq) libraries were prepared by the Max Planck Genome Centre Cologne (Germany) using the Illumina TruSeq stranded RNA sample preparation kit and were subjected to single-end (Isolate K1) or paired-end (all other isolates) sequencing (100-bp reads) by using the Illumina HiSeq2500 Sequencing System. To make sure the sequencing reads were of sufficiently high quality, we performed an initial quality check of the sequence data using the FastQC suite (www.bioinformatics.babraham.ac.uk/projects/fastqc/). Subsequently, the RNA-seq reads were mapped to the *Bgh* DH14 BluGen (www.blugen.org) genome assembly (Version 3.0) under consideration of exon-intron structures using the splice aware aligner Tophat2 (68) with settings -a 10, -g 10, -r 160,–mate-std-dev 160 and providing known splice sites based on the BluGen gene models from July 2012 (a corresponding gff-file can be obtained from www.mpipz.mpg.de/23693/Powdery_Mildews).

To assess the expression levels of individual genes, we obtained fragment counts per gene for each isolate from the mapped RNA-seq reads of both time points using the htseq-count script (s = reverse, t = exon) in the package HTSeq (69). In parallel, SNPs were identified from the mapped RNA-seq reads by using the mpileup function in the SAMtools toolkit (Version 0.1.18) (70). This SNP calling was performed on the alignment data of the individual isolates (with options -A and -u) and on a combined alignment dataset for all isolates (with options -A, -u, -D, -d 2000) that was obtained by merging the mapped RNA-seq reads from all isolates using SAMtools merge. The resulting SNP sets were filtered by using SnpSift (Version 3.4) (71) to extract high-quality variants with sufficient read coverage (coverage of at least 3 reads for individual isolates or at least 30 reads for the combined dataset), a SNP calling quality score of at least 50, a genotype quality score of at least 10, no significant evidence for strand bias (at $P < 1e^{-10}$) or tail distance bias (at $P < 1e^{-5}$), and where the alternate allele was present in at least half of the reads of one isolate (alternate allele frequency of at least 50% for individual isolates or at least 3.3% for the combined dataset). Subsequent variant annotation and effect prediction was performed by using snpEff (Version 3.4; default settings) (72) based on the DH14 gene models.

The RNA-seq data used in this study are deposited in the National Center for Biotechnology Information Gene Expression Omnibus database (accession no. GSE83237).

Population Structure Analysis of *Bgh* Isolates. To obtain a suitable SNP set for population structure analysis, we further filtered the set of high-quality SNPs obtained from the combined alignment data as described above and extracted only silent (synonymous) SNPs in coding regions, for which exactly two different alleles were found (diallelic SNPs) and complete genotype information was available for all isolates (i.e., no missing data). The resulting set of 5,049 high-quality diallelic synonymous SNPs was used to examine the genotype data for the presence of any obvious population structure using the R packages adegenet (Version 2.0.1) (73) and ape (Version 3.4) (74), To this end, we created a PCA plot from the genotype data using the function glPca (R package adegenet) and additionally computed a neighbor-joining tree based on the pairwise Euclidean distances between the isolate genotypes using the function nj (R package ape). The SNP locations for each sequenced isolate with respect to the 15 largest contigs of the DH14 reference genome were visualized by using Circos (Version 0.62.1) (75)

Genetic Association Analysis. Because the highly divergent genotype observed for isolate RACE1 could conceal existing associations, this isolate was not included for the actual association screening. Therefore, we identified SNPs from the combined alignment data of all isolates except RACE1 and extracted a set of 67,385 high-confidence SNPs, for which the alternate allele was supported by at least 10% of the mapped sequencing reads and otherwise using the same criteria as described above. From this set, we further extracted those 6,982 diallelic SNPs that were predicted to introduce nonsynonymous substitutions in the predicted reference proteins and tested each of these SNPs for their association with the observed avirulence phenotypes using Fisher's exact test. Moreover, we also wanted to be able to detect potential candidates for which the loss of avirulence might be caused, not by one common SNP in all isolates, but by different isolate-specific SNPs. Therefore, we additionally integrated all high-confidence nonsynonymous SNPs over each gene and also tested these genewise collapsed variants for association with the observed avirulence phenotypes using Fisher's exact test. The association test and genewise integration of SNPs were implemented in R (code available upon request). To predict protein structures of the identified AVR_A candidates, the respective amino acids were submitted to the IntFOLD (38), I-TASSER (39), and HHpred (37) servers using default settings.

Generation of Expression Constructs. RNA isolated from barley leaves challenged with *Bgh* isolates DH14, A6, CC52, and RACE1 was used for cDNA synthesis using SuperScript II Reverse Transcriptase (Thermo Fisher Scientific). Subsequently, the cDNA sequences of the effector genes AVR_{a1}, AVR_{a1}-*V1*, -*V2*, AVR_{a13}-*1*, -*3*, -*V1*, and -*V2* without signal peptide sequences were PCR-amplified by using the primers listed in Table S3. The PCR products were first cloned into pENTR-D/TOPO (Thermo Fisher Scientific) and then into the binary vector pIPKb002, which contains the maize (*Zea mays*) ubiquitin 1 promoter (40). To introduce a single FLAG-tag at the C terminus, the corresponding nucleotide sequence was added at the 3′ end of AVR_{A1}, AVR_{a1}-*V1*, and -*V2* in the pENTR-D/TOPO. To introduce a single FLAG-tag at the N terminus, the corresponding sequence was added at the 5′ end of AVR_{a13}-*1*, -*3*, -*V1*, and -*V2* in the pENTR-D/TOPO. The resulting entry clones were transferred into pIPKb002. Constructs were used in the transient gene expression assays in barley leaves or barley protoplasts as described below. To generate transgenic *Arabidopsis* plants expressing AVR_{a1}, the AVR_{a1} gene without the signal peptide sequence was cloned together with the *Arabidopsis* poly-ubiquitin promoter (AtPubiq10) into the binary vector R4pGWB4-stop-HSP, which contains the HSP terminator to increase the gene expression (76).

Transient Gene Expression by *Agrobacterium*-Mediated Transformation of Barley Leaves. The binary overexpression vector pIPKb002 and *Agrobacterium tumefaciens* strain AGL1 were used for transient expression of effectors. Fresh *Agrobacteria* were grown overnight in yeast extract broth (YEB) medium with rifampicin, carbenicillin, and spectinomycin. After centrifugation, bacterial pellets were resuspended in an infiltration buffer containing 10 mM Mes, 10 mM $MgCl_2$, and 400 μM acetosyringone to an optical density of 2.0. The *Agrobacterium* suspension was infiltrated into the adaxial side of the second leaf of 12-d-old barley plants by using a 1-mL syringe without needle. Plant phenotypes were examined at between 5 and 14 d after infiltration.

Transient Gene Expression and Cell Death Assay in Barley Protoplasts. Isolation of barley protoplast was adapted from an established *Arabidopsis* protoplast isolation method (41) with the following modifications: (*i*) The enzyme solution consisted of 10 mM Mes (pH 5.7), 1.5% (wt/vol) cellulase R10, 0.5% macerozyme R10, 0.6 M mannitol, 20 mM KCl, 10 mM $CaCl_2$, and 0.1% BSA. (*ii*) The concentration of mannitol in the solution W1 was 0.6 M (instead of 0.4 M). (*iii*) Epidermis of the first leaves of 7-d-old plants was peeled (instead of chopping leaves), and then leaves without epidermis were immersed into the enzyme solution to release mesophyll protoplasts. After isolation of barley protoplasts, 7.5 μg of the luciferase reporter plasmid and 7.5 μg of the respective effector construct in a volume of 30 μL were cotransfected into 300-μL barley protoplasts by using the PEG–calcium-mediated DNA transfection method (41). At 16 h after transfection, protoplasts were collected by centrifugation, dissolved in Luciferase Cell Culture Lysis buffer (Promega, catalog no. E1531), and then the luciferase activity was measured by using the Luciferase Assay System (Promega, catalog no. E1501).

Protein Analysis. To examine effector protein expression in barley protoplasts, the FLAG-tagged effector constructs were transfected into protoplasts isolated

from barley cv. Golden Promise or Manchuria. At 18 h after transfection, protoplasts were collected by centrifugation and dissolved in protein lysis buffer containing 50 mM Tris·HCl (pH 7.5), 1 mM EDTA (pH 7.5), 150 mM NaCl, 10% (vol/vol) glycerol, 10 mM NaF, 1 mM Na_2VO_4, 25 mM β-glycerophosphate, 10 mM DTT, 1% Triton X-100, and protease inhibitors (Roche, catalog no. 11836145001). Protein samples were loaded onto an 18% gel for Western blotting and probed with mouse monoclonal anti-FLAG M2 (Sigma-Aldrich, catalog no. F3165), followed by goat anti-mouse IgG-HRP (Santa Cruz, catalog no. sc-2005) to detect the FLAG-tagged effector proteins.

Generation of Stable Transgenic *A. thaliana*. Two of 15 T_1 plants, designated AVR_{a1} line P4-2 and AVR_{a1} line P4-4, accumulated high levels of AVR_{a1} transcript. Two of 16 T_1 plants (designated AVR_{a1}–*FLAG*-12 and AVR_{a1}–*FLAG*-14) accumulated detectable AVR_{A1}–FLAG protein, whereas 7 of 14 transgenic T_1 plants accumulated detectable AVR_{A1}–V1-FLAG protein (designated AVR_{a1}-*V1-FLAG*-1, -2, -3, -4, -6, -9, and -14). We chose to cross AVR_{a1} P4-2, AVR_{a1} P4-4, AVR_{a1}–*FLAG*-12, AVR_{a1}–*FLAG*-14, AVR_{a1}–*V1-FLAG*-1, and AVR_{a1}–*V1-FLAG*-2 T_1 plants with transgenic *A. thaliana* plants (line 47-2) homozygous for the *Mla1* transgene (25). The line 47-2 was crossed as the female parent. Transgene segregation analysis among the T_2 progeny suggested that the AVR_{a1} P4-2, AVR_{a1} P4-4, AVR_{a1}–*FLAG*-14, and AVR_{a1}–*V1-FLAG*-2 carried a single copy heterozygous integration of the respective transgenes. The segregation analysis of AVR_{a1}–*FLAG*-12 and AVR_{a1}–*V1-FLAG*-1 suggested two or more copies of the respective transgene.

MCL Analysis. To identify orthologs of AVR_{A1} and AVR_{A13} in *Bgt* and define CSEP families across the two species, groups of orthologous proteins were inferred from the *Bgh* and *Bgt* CSEPs by using OrthoMCL (Version 2.0) (46) with standard parameters and granularity 1.5 for the MCL clustering step. Because we observed that AVR_{A1} and AVR_{A13} are able to induce the MLA-dependent cell death response without the signal peptide, the OrthoMCL clustering was performed on the respective *Bgh* and *Bgt* protein sequences after removal of the signal peptides by using SignalP (Version 4.1) (77) with a D value cutoff of 0.2.

Subsequently, we extracted the two OrthoMCL families containing AVR_{A1} and AVR_{A13} and performed a multiple sequence alignment of the respective protein sequences without the signal peptides using Clustal Omega (78) and visualized the alignments. Moreover, to check for the presence of the respective *Bgt* family members in three further *Bgt* isolates with published genome sequences, we performed a Blast search with the respective CDS sequences against the genome assemblies to identify the respective genome contigs. Subsequently, we manually extracted the genomic sequences of the respective regions in the different isolates and used MEGA (Version 5) (79) to perform a codon-based nucleotide alignment with Muscle (default settings) on the CDS sequences and corresponding genomic regions. After manual fine-tuning, the respective nucleotide alignments were visualized with Geneious Basic (Version 5.0.3) (80).

ACKNOWLEDGMENTS. We thank L. Chartrain and J. Brown (John Innes Centre) for providing the *Bgh* isolates DH14, CC1, CC52, CC66, CC88, CC107, and CC148; M. F. Lyngkjær (University of Copenhagen) for *Bgh* isolate B103; R. Oliver (Curtin University) for the *Bgh* isolates Aby, Art, and Will; H. Hisano (Okayama University) for the *Bgh* isolate OU14; N. Yamaoka (Ehime University) for the *Bgh* isolate RACE1; and M. Moscou (The Sainsbury Laboratory) for providing the Manchuria NIL lines. The ZmUbi-*LUC* plasmid, pIPKb002, and R4pGWB4-stop-HSP were kindly provided by R. Panstruga (RWTH Aachen University), J. Kumlehn (Leibniz Institute of Plant Genetics and Crop Plant Research), and N. Mitsuda (National Institute of Advanced Industrial Science and Technology), respectively. We thank C. Pedersen (University of Copenhagen) for helpful suggestions. We also thank S. Haigis and M. Yoshikawa-Maekawa for maintaining the *Bgh* isolates; P. Köchner for technical assistance; and the Max Planck Genome Centre Cologne for RNA-seq. This work was supported by the Max-Planck Society (X.L., B.K., I.M.L.S., S.B. and P.S.-L.); German Research Foundation in the Collaborative Research Centre Grant SFB670 (to B.K., T.M., and P.S.-L.); Grains Research & Development Corporation Projects CUR00017 and CUR00023 P8 (to S.R.E.); and the JSPS KAKENHI Grant JP16K07618 Inamori Foundation (to T.Y.).

1. Zipfel C (2014) Plant pattern-recognition receptors. *Trends Immunol* 35(7):345–351.
2. Jacob F, Vernaldi S, Maekawa T (2013) Evolution and conservation of plant NLR functions. *Front Immunol* 4:297.
3. Maekawa T, Kufer TA, Schulze-Lefert P (2011) NLR functions in plant and animal immune systems: So far and yet so close. *Nat Immunol* 12(9):817–826.
4. Meyers BC, Kaushik S, Nandety RS (2005) Evolving disease resistance genes. *Curr Opin Plant Biol* 8(2):129–134.
5. Ellis JG, Lawrence GJ, Luck JE, Dodds PN (1999) Identification of regions in alleles of the flax rust resistance gene L that determine differences in gene-for-gene specificity. *Plant Cell* 11(3):495–506.
6. Allen RL, et al. (2004) Host-parasite coevolutionary conflict between *Arabidopsis* and downy mildew. *Science* 306(5703):1957–1960.
7. Srichumpa P, Brunner S, Keller B, Yahiaoui N (2005) Allelic series of four powdery mildew resistance genes at the Pm3 locus in hexaploid bread wheat. *Plant Physiol* 139(2):885–895.
8. Bhullar NK, Zhang Z, Wicker T, Keller B (2010) Wheat gene bank accessions as a source of new alleles of the powdery mildew resistance gene Pm3: A large scale allele mining project. *BMC Plant Biol* 10(1):88.
9. Seeholzer S, et al. (2010) Diversity at the Mla powdery mildew resistance locus from cultivated barley reveals sites of positive selection. *Mol Plant Microbe Interact* 23(4): 497–509.
10. Kanzaki H, et al. (2012) Arms race co-evolution of *Magnaporthe oryzae* AVR-Pik and rice Pik genes driven by their physical interactions. *Plant J* 72(6):894–907.
11. Dodds PN, et al. (2006) Direct protein interaction underlies gene-for-gene specificity and coevolution of the flax resistance genes and flax rust avirulence genes. *Proc Natl Acad Sci USA* 103(23):8888–8893.
12. Hall SA, et al. (2009) Maintenance of genetic variation in plants and pathogens involves complex networks of gene-for-gene interactions. *Mol Plant Pathol* 10(4): 449–457.
13. Glawe DA (2008) The powdery mildews: A review of the world's most familiar (yet poorly known) plant pathogens. *Annu Rev Phytopathol* 46:27–51.
14. Thordal-Christensen H, Gregersen PL, Collinge DB (2000) The barley/Blumeria (Syn. Erysiphe) Graminis interaction. *Mechanisms of Resistance to Plant Diseases*, eds Slusarenko AJ, Fraser RSS, van Loon LC (Springer, Dordrecht, The Netherlands), pp 77–100.
15. Spanu PD, et al. (2010) Genome expansion and gene loss in powdery mildew fungi reveal tradeoffs in extreme parasitism. *Science* 330(6010):1543–1546.
16. Pedersen C, et al. (2012) Structure and evolution of barley powdery mildew effector candidates. *BMC Genomics* 13(1):694.
17. Hacquard S, et al. (2013) Mosaic genome structure of the barley powdery mildew pathogen and conservation of transcriptional programs in divergent hosts. *Proc Natl Acad Sci USA* 110(24):E2219–E2228.
18. Wicker T, et al. (2013) The wheat powdery mildew genome shows the unique evolution of an obligate biotroph. *Nat Genet* 45(9):1092–1096.
19. Middleton CP, et al. (2014) Sequencing of chloroplast genomes from wheat, barley, rye and their relatives provides a detailed insight into the evolution of the Triticeae tribe. *PLoS One* 9(3):e85761.
20. Jørgensen JH, Wolfe M (1994) Genetics of powdery mildew resistance in barley. *Crit Rev Plant Sci* 13(1):97–119.
21. Brunner S, et al. (2010) Intragenic allele pyramiding combines different specificities of wheat Pm3 resistance alleles. *Plant J* 64(3):433–445.
22. Periyannan S, et al. (2013) The gene Sr33, an ortholog of barley Mla genes, encodes resistance to wheat stem rust race Ug99. *Science* 341(6147):786–788.
23. Mago R, et al. (2015) The wheat Sr50 gene reveals rich diversity at a cereal disease resistance locus. *Nat Plants* 1:15186.
24. Zhou F, et al. (2001) Cell-autonomous expression of barley Mla1 confers race-specific resistance to the powdery mildew fungus via a Rar1-independent signaling pathway. *Plant Cell* 13(2):337–350.
25. Maekawa T, Kracher B, Vernaldi S, Ver Loren van Themaat E, Schulze-Lefert P (2012) Conservation of NLR-triggered immunity across plant lineages. *Proc Natl Acad Sci USA* 109(49):20119–20123.
26. Bourras S, McNally KE, Müller MC, Wicker T, Keller B (2016) Avirulence genes in cereal powdery mildews: The gene-for-gene hypothesis 2.0. *Front Plant Sci* 7:241.
27. Amselem J, et al. (2015) Evolution of the EKA family of powdery mildew avirulence-effector genes from the ORF 1 of a LINE retrotransposon. *BMC Genomics* 16(1):917.
28. Ridout CJ, et al. (2006) Multiple avirulence paralogues in cereal powdery mildew fungi may contribute to parasite fitness and defeat of plant resistance. *Plant Cell* 18(9):2402–2414.
29. Pedersen C, Rasmussen SW, Giese H (2002) A genetic map of *Blumeria graminis* based on functional genes, avirulence genes, and molecular markers. *Fungal Genet Biol* 35(3):235–246.
30. Moseman JG (1972) Isogenic barley lines for reaction to *Erysiphe graminis F. Sp. Hordei*. *Crop Sci* 12(5):681–682.
31. Wei F, et al. (1999) The Mla (powdery mildew) resistance cluster is associated with three NBS-LRR gene families and suppressed recombination within a 240-kb DNA interval on chromosome 5S (1HS) of barley. *Genetics* 153(4):1929–1948.
32. Halterman DA, Wei F, Wise RP (2003) Powdery mildew-induced Mla mRNAs are alternatively spliced and contain multiple upstream open reading frames. *Plant Physiol* 131(2):558–567.
33. Wei F, Wing RA, Wise RP (2002) Genome dynamics and evolution of the Mla (powdery mildew) resistance locus in barley. *Plant Cell* 14(8):1903–1917.
34. Hiura U, Heta H (1955) Studies on the disease-resistance in barley III. Further studies on the physiologic races of *erysiphe graminis hordei* in Japan. *Berichte des Ohara Instituts für Landwirtschaftliche Biologie* 10:135–152.
35. Robinson JT, et al. (2011) Integrative genomics viewer. *Nat Biotechnol* 29(1):24–26.
36. Thorvaldsdóttir H, Robinson JT, Mesirov JP (2013) Integrative Genomics Viewer (IGV): High-performance genomics data visualization and exploration. *Brief Bioinform* 14(2):178–192.

37. Söding J, Biegert A, Lupas AN (2005) The HHpred interactive server for protein homology detection and structure prediction. *Nucleic Acids Res* 33(Web Server issue): W244–W248.
38. McGuffin LJ, Atkins JD, Salehe BR, Shuid AN, Roche DB (2015) IntFOLD: An integrated server for modelling protein structures and functions from amino acid sequences. *Nucleic Acids Res* 43(Web Server issue):W169–W173.
39. Yang J, et al. (2015) The I-TASSER suite: Protein structure and function prediction. *Nat Methods* 12(1):7–8.
40. Himmelbach A, et al. (2007) A set of modular binary vectors for transformation of cereals. *Plant Physiol* 145(4):1192–1200.
41. Yoo S-D, Cho Y-H, Sheen J (2007) *Arabidopsis* mesophyll protoplasts: A versatile cell system for transient gene expression analysis. *Nat Protoc* 2(7):1565–1572.
42. Xiang T, et al. (2008) Pseudomonas syringae effector AvrPto blocks innate immunity by targeting receptor kinases. *Curr Biol* 18(1):74–80.
43. Fraiture M, Zheng X, Brunner F (2014) An Arabidopsis and tomato mesophyll protoplast system for fast identification of early MAMP-triggered immunity-suppressing effectors. *Plant-Pathogen Interactions: Methods and Protocols*, eds Birch P, Jones TJ, Bos IBJ (Humana, Totowa, NJ), pp 213–230.
44. Yoshida K, et al. (2009) Association genetics reveals three novel avirulence genes from the rice blast fungal pathogen *Magnaporthe oryzae*. *Plant Cell* 21(5):1573–1591.
45. Bieri S, et al. (2004) RAR1 positively controls steady state levels of barley MLA resistance proteins and enables sufficient MLA6 accumulation for effective resistance. *Plant Cell* 16(12):3480–3495.
46. Li L, Stoeckert CJ, Jr, Roos DS (2003) OrthoMCL: Identification of ortholog groups for eukaryotic genomes. *Genome Res* 13(9):2178–2189.
47. Menardo F, et al. (2016) Hybridization of powdery mildew strains gives rise to pathogens on novel agricultural crop species. *Nat Genet* 48(2):201–205.
48. Sato K, et al. (2016) Improvement of barley genome annotations by deciphering the Haruna Nijo genome. *DNA Res* 23(1):21–28.
49. Lyngkj ÆR MF, Jensen HP, Østergård H (1995) A Japanese powdery mildew isolate with exceptionally large infection efficiency on Mlo-resistant barley. *Plant Pathol* 44(5):786–790.
50. Zhang S, et al. (2015) Function and evolution of *Magnaporthe oryzae* avirulence gene AvrPib responding to the rice blast resistance gene Pib. *Sci Rep* 5:11642.
51. Panstruga R, Dodds PN (2009) Terrific protein traffic: The mystery of effector protein delivery by filamentous plant pathogens. *Science* 324(5928):748–750.
52. Shen QH, et al. (2007) Nuclear activity of MLA immune receptors links isolate-specific and basal disease-resistance responses. *Science* 315(5815):1098–1103.
53. Shen QH, et al. (2003) Recognition specificity and RAR1/SGT1 dependence in barley Mla disease resistance genes to the powdery mildew fungus. *Plant Cell* 15(3):732–744.
54. Dodds PN, Lawrence GJ, Catanzariti A-M, Ayliffe MA, Ellis JG (2004) The *Melampsora lini* AvrL567 avirulence genes are expressed in haustoria and their products are recognized inside plant cells. *Plant Cell* 16(3):755–768.
55. Weßling R, et al. (2014) Convergent targeting of a common host protein-network by pathogen effectors from three kingdoms of life. *Cell Host Microbe* 16(3):364–375.
56. Mukhtar MS, et al.; European Union Effectoromics Consortium (2011) Independently evolved virulence effectors converge onto hubs in a plant immune system network. *Science* 333(6042):596–601.
57. Maqbool A, et al. (2015) Structural basis of pathogen recognition by an integrated HMA domain in a plant NLR immune receptor. *eLife* 4:e08709.
58. de Guillen K, et al. (2015) Structure analysis uncovers a highly diverse but structurally conserved effector family in phytopathogenic fungi. *PLoS Pathog* 11(10):e1005228.
59. Win J, et al. (2012) Sequence divergent RXLR effectors share a structural fold conserved across plant pathogenic oomycete species. *PLoS Pathog* 8(1):e1002400.
60. Zhang X, Henriques R, Lin S-S, Niu Q-W, Chua N-H (2006) Agrobacterium-mediated transformation of *Arabidopsis thaliana* using the floral dip method. *Nat Protoc* 1(2): 641–646.
61. Hinze K, Thompson RD, Ritter E, Salamini F, Schulze-Lefert P (1991) Restriction fragment length polymorphism-mediated targeting of the ml-o resistance locus in barley (*Hordeum vulgare*). *Proc Natl Acad Sci USA* 88(9):3691–3695.
62. Sherwood JE, Slutsky B, Somerville SC (1991) Induced morphological and virulence variants of the obligate barley pathogen *Erysiphe graminis* f. sp. *hordei*. *Phytophathology* 81:1350–1357.
63. Wiberg A (1974) Genetical studies of spontaneous sources of resistance to powdery mildew in barley. *Hereditas* 77(1):89–148.
64. Wiberg A (1974) Sources of resistance to powdery mildew in barley. *Hereditas* 78(1): 1–40.
65. Brown JKM, Jessop AC, Thomas S, Rezanoor HN (1992) Genetic control of the response of *Erysiphe graminis f.sp. hordei* to ethirimol and triadimenol. *Plant Pathol* 41(2):126–135.
66. Brown JKM, Wolfe MS (1990) Structure and evolution of a population of *Erysiphe graminis f.sp. hordei*. *Plant Pathol* 39(3):376–390.
67. Kølster P, Munk L, Stølen O, Løhde J (1986) Near-isogenic barley lines with genes for resistance to powdery mildew1. *Crop Sci* 26(5):903–907.
68. Kim D, et al. (2013) TopHat2: Accurate alignment of transcriptomes in the presence of insertions, deletions and gene fusions. *Genome Biol* 14(4):R36.
69. Anders S, Pyl PT, Huber W (2015) HTSeq—a Python framework to work with high-throughput sequencing data. *Bioinformatics* 31(2):166–169.
70. Li H, et al.; 1000 Genome Project Data Processing Subgroup (2009) The Sequence Alignment/Map format and SAMtools. *Bioinformatics* 25(16):2078–2079.
71. Cingolani P, et al. (2012) Using Drosophila melanogaster as a model for genotoxic chemical mutational studies with a new program, SnpSift. *Front Genet* 3:35.
72. Cingolani P, et al. (2012) A program for annotating and predicting the effects of single nucleotide polymorphisms, SnpEff: SNPs in the genome of Drosophila melanogaster strain w1118; iso-2; iso-3. *Fly (Austin)* 6(2):80–92.
73. Jombart T, Ahmed I (2011) adegenet 1.3-1: New tools for the analysis of genome-wide SNP data. *Bioinformatics* 27(21):3070–3071.
74. Paradis E, Claude J, Strimmer K (2004) APE: Analyses of Phylogenetics and Evolution in R language. *Bioinformatics* 20(2):289–290.
75. Krzywinski M, et al. (2009) Circos: An information aesthetic for comparative genomics. *Genome Res* 19(9):1639–1645.
76. Oshima Y, et al. (2011) Novel vector systems to accelerate functional analysis of transcription factors using chimeric repressor gene-silencing technology (CRES-T). *Plant Biotechnol* 28(2):201–210.
77. Petersen TN, Brunak S, von Heijne G, Nielsen H (2011) SignalP 4.0: Discriminating signal peptides from transmembrane regions. *Nat Methods* 8(10):785–786.
78. Sievers F, et al. (2011) Fast, scalable generation of high-quality protein multiple sequence alignments using Clustal Omega. *Mol Syst Biol* 7:539.
79. Tamura K, et al. (2011) MEGA5: Molecular evolutionary genetics analysis using maximum likelihood, evolutionary distance, and maximum parsimony methods. *Mol Biol Evol* 28(10):2731–2739.
80. Kearse M, et al. (2012) Geneious Basic: An integrated and extendable desktop software platform for the organization and analysis of sequence data. *Bioinformatics* 28(12):1647–1649.

Supporting Information

Lu et al. 10.1073/pnas.1612947113

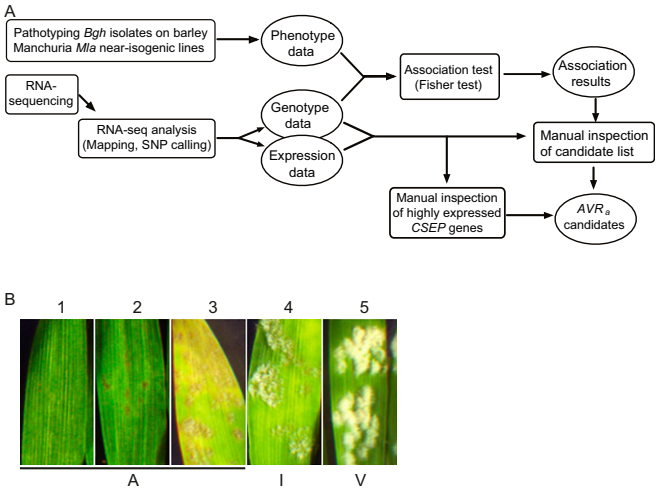

Fig. S1. Workflow of the genetic association analysis and infection types of the barley powdery mildew. (*A*) Schematic representation of the genetic association analysis workflow that was applied in this study to identify AVR_a candidates. Briefly, phenotype and genotype data were obtained and subjected to statistical analysis (Fisher's exact test) to identify candidate loci/genes for which the observed allele frequencies were associated with the observed pathotypes. To identify AVR_a candidates, additionally differences in gene expression levels were taken into account, and potential candidate loci were inspected manually by using the IGV. (*B*) Infection types (ITs) at 9 d after spore inoculation on detached barley leaves. ITs ranged from undetectable *Bgh* colony formation without and with patches of leaf cell death (IT 1 and 2, respectively), restricted colony formation with underlying cell death patches (IT 3), to unrestricted colony formation with or without leaf chlorosis (IT 4 and 5, respectively) (9). ITs 1–3 were rated as avirulent interactions (A); IT 4 and 5 were rated as intermediate (I) and virulent interactions (V), respectively.

Fig. S2. Circular visualization of SNP distributions for 16 *Bgh* isolates with respect to the DH14 reference genome. The outermost track represents the 15 largest *Bgh* DH14 contigs (scale: kilobases) with the locations of annotated genes highlighted in dark gray. The other tracks mark in color the locations of SNPs vs. DH14 in the other isolates colored by geographic origin: Japanese isolates in green, Australian isolates in yellow, North American isolates in dark blue, and European isolates in ruby. Areas of low/no sequencing coverage (less than three reads) are marked in gray in the SNP tracks. The two highlighted regions (I and II) that we found to be relatively conserved (low number of SNPs) among all isolates except RACE1 (I) or among the European isolates (II) are consistent with previously identified monomorphic blocks between DH14, A6, and K1 (II) (17).

Fig. S3. (*A* and *B*) Nucleotide sequences of AVR_{a1} (*A*) and AVR_{a13} (*B*) and their variants. Nucleotides shown in red indicate sequence differences compared with the reference CDS sequences. (*C*) Identified DNA fragment inserted into the AVR_{a13} locus of isolate B103.

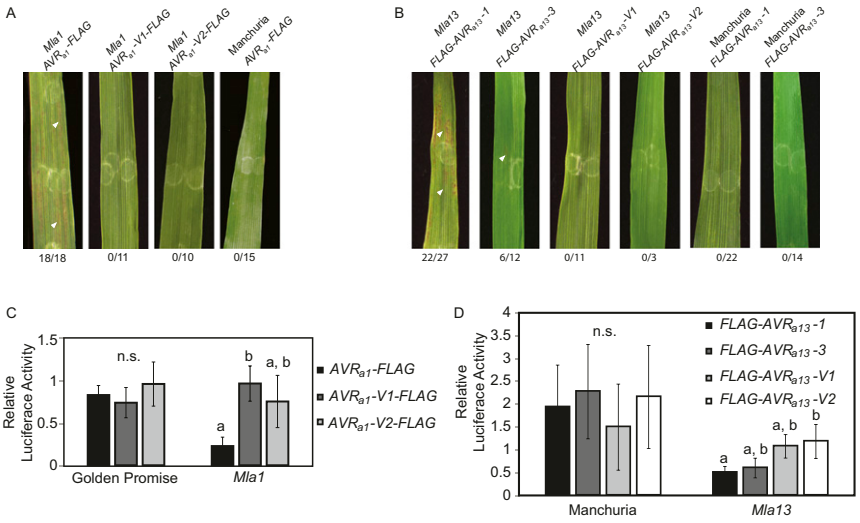

Fig. S4. Transient expression of the epitope-tagged AVR_{A1} and AVR_{A13} in barley triggers cell death in genotypes carrying cognate *Mla* recognition specificities. (*A* and *B*) Expression cassettes for *AVR_{a1}-FLAG*, *AVR_{a1}-V1-FLAG*, and *AVR_{a1}-V2-FLAG* (*A*) or *FLAG-AVR_{a13}-1*, *FLAG-AVR_{a13}-3*, *FLAG-AVR_{a13}-V1*, and *FLAG-AVR_{a13}-V2* (*B*) without signal peptides were delivered into barley leaves by *Agrobacterium* infiltration. (*A*) Expression of *AVR_{a1}-FLAG*, but not *AVR_{a1}-V1-FLAG* or *AVR_{a1}-V2-FLAG*, induces a specific cell death response in an *Mla1* NIL, but not in *Mla13* and *Mla6* NILs or Manchuria. (*B*) Expression of *FLAG-AVR_{a13}-1* and *FLAG-AVR_{a13}-3*, but not *FLAG-AVR_{a13}-V1* or *FLAG-AVR_{a13}-V2*, induces a specific cell death response in an *Mla13* NIL, but not in *Mla1* and *Mla15* NILs or Manchuria. White arrows indicate necrotic leaf patches. Incidence of infiltrated leaves with cell death response is indicated for each genotype. (*C* and *D*) Relative luciferase activity after transformation of *AVR_{a1}-FLAG*, *AVR_{a1}-V1-FLAG*, and *AVR_{a1}-V2-FLAG* into barley protoplasts generated from Golden Promise or *Mla1* transgenic plants (*C*) or transformation of *FLAG-AVR_{a13}-1*, *FLAG-AVR_{a13}-3*, *FLAG-AVR_{a13}-V1*, and *FLAG-AVR_{a13}-V2* into barley protoplasts generated from Manchuria or *M1a13* NIL (*D*). Luciferase activity was normalized for each plant line by setting the detected luminescence for the corresponding empty vector transfection to 1. For each plant genotype, differences between samples were assessed by using ANOVA and subsequent Tukey post hoc tests. Observed ANOVA *P* values were as follows: Golden promise: $P = 0.43$; *Mla1*: $P = 0.02$ (*C*); Manchuria: $P = 0.79$; *Mla13*: $P = 0.03$ (*D*). Samples marked by identical letters in the plot did not differ significantly ($P < 0.05$) in the Tukey test for the corresponding genotype. n.s., not significant.

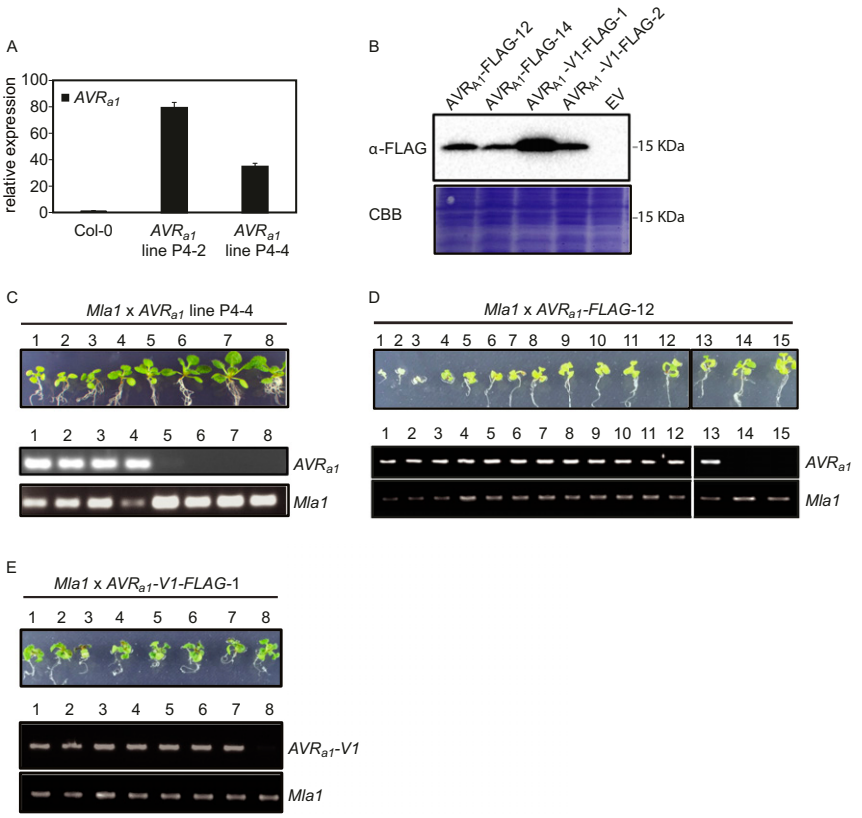

Fig. S5. AVR_{A1} is recognized by barley MLA1 in stable transgenic *Arabidopsis* plants. (*A*) Expression levels of AVR_{a1} in AVR_{a1} P4-2 and AVR_{a1} P4-2 T_1 plants. (*B*) Protein levels of AVR_{A1}-FLAG or AVR_{A1}-V1-FLAG in the respective T_2 plants. (*C–E*) Seedling growth of the F_1 progenies from crosses between homozygous *A. thaliana* plants carrying *Mla1* (25) and T_1 plants carrying constructs for the expression of AVR_{a1} (*C*), AVR_{a1}-*FLAG* (*D*), or AVR_{a1}-*V-FLAG* (*E*). F_1 progenies were ordered by plant size when possible. Seedlings were grown on solid 1/2 MS media for 14–16 d before the examination of seedling growth. The corresponding segregation patterns of the transgenes are shown in the lower panels.

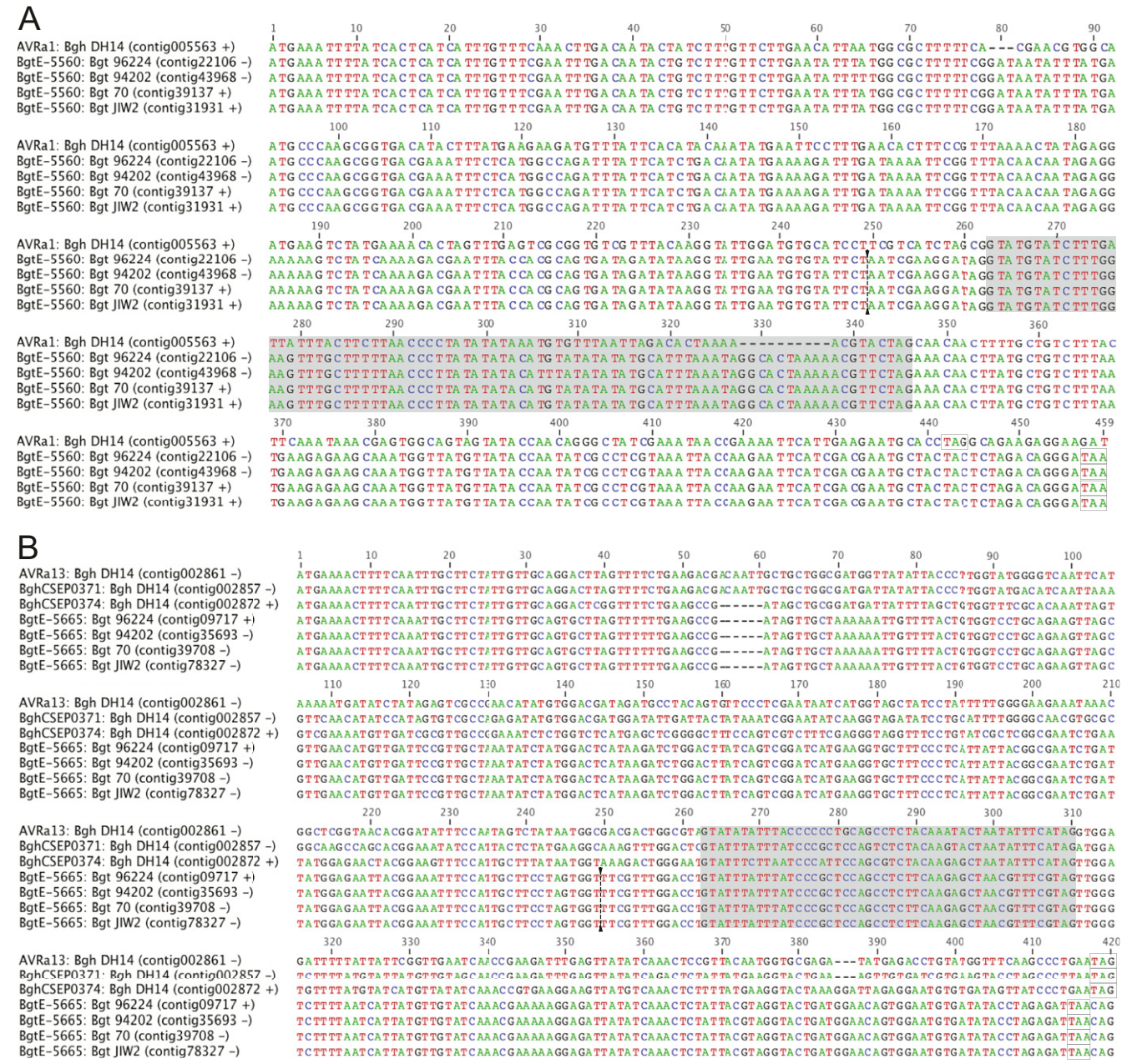

Fig. S6. Genomic sequence alignment of AVR_{a1} and AVR_{a13} families. Nucleotide sequences of the *Bgh* and *Bgt* genomic regions representing the members of the AVR_{a1} (*A*) and AVR_{a13} (*B*) *CSEP* families were aligned based on the genome sequences of *Bgh* isolate DH14 and *Bgt* isolates 96224, 94202, 70, and JW2. Presumed intronic regions in the alignment are shaded in gray; predicted stop codons are surrounded by a black box; and the position where the published *Bgt* annotations end are marked by a black line.

Table S1. *Bgh* isolates used for association test

			Infection phenotypes on barley NILs					
			Mla1	*Mla6*	*Mla7*	*Mla10*	*Mla13*	*Mla15*
Isolates	Origin	Mating locus	CI 16137	CI 16151	CI 16147	CI 16149	CI 16155	CI 16153
DH14	UK	*MAT1-2*	1	1	2	5	1	2
CC1	UK	*MAT1-2*	1	1	2	2	1	1
CC52	UK	*MAT1-1*	1	2	5	5	5	5
CC66	UK	*MAT1-1*	1	5	5	5	1	5
CC88	UK	*MAT1-2*	5	1	5	4	1	5
CC107	UK	*MAT1-1*	2	1	5	5	2	5
CC148	UK	*MAT1-1*	1	5	3	3	2	3
K1	Germany	*MAT1-2*	1	5	5	5	1	5
A6	Denmark	*MAT1-1*	5	1	3	3	1	1
B103	Denmark	*MAT1-1*	1	5	5	3	5	5
63.5	US	*MAT1-2*	1	1	2	1	1	3
NCI	US	*MAT1-2*	5	1	1	2	1	1
Aby	Australia	*MAT1-1*	1	1	2	2	1	2
Art	Australia	*MAT1-2*	1	1	3	2	1	2
Will	Australia	*MAT1-2*	1	1	3	3	1	1
OU14	Japan	*MAT1-2*	1	1	1	3	1	1
RACE1	Japan	*MAT1-1*	5	1	1	2	1	1

Observed barley near-isogenic Manchuria lines response against *Bgh* isolates were scored 9 d after inoculation and grouped into five ITs: IT1, full resistance with undetectable fungal growth; IT2, rarely detected fungal growth and detectable necrotic patches on the leave; IT3, occasionally fungal hyphae growth surrounded by necrotic patches; IT4, detectable fungal growth and sporulation with necrotic patches; and IT5, massive fungal growth and sporulation without detectable necrotic areas (also shown in Fig. S1).

Table S2. Summary statistics of RNA-sequencing read alignment and SNP calling for the collection of *Bgh* isolates against isolate DH14

			Fragments sequenced			Aligned to DH14 genome				
Isolate	Material	Sequencing mode	16 h	48 h	Total	16 h	48 h	Total	No. of SNPs, total*	No. of SNPs, after filtering†
NCI	Whole leaf	Paired-end	50,154,753	51,426,484	101,581,237	304,804	162,771	467,575	21,293	8,246
63.5	Whole leaf	Paired-end	51,404,046	51,575,361	102,979,407	604,519	3,583,877	4,188,396	59,303	26,495
CC1	Whole leaf	Paired-end	50,976,431	51,163,669	102,140,100	314,833	1,453,047	1,767,880	40,190	18,061
CC66	Whole leaf	Paired-end	55,775,614	52,225,048	108,000,662	143,447	3,754,328	3,897,775	51,035	21,341
CC88	Whole leaf	Paired-end	55,054,230	50,669,586	105,723,816	181,650	317,459	499,109	20,650	8,008
CC107	Whole leaf	Paired-end	50,013,990	48,674,527	98,688,517	190,932	1,323,261	1,514,193	31,202	13,832
CC52	Whole leaf	Paired-end	52,361,338	57,025,784	109,387,122	188,006	377,544	565,550	22,695	7,613
CC148	Whole leaf	Paired-end	49,641,971	56,570,523	106,212,494	157,735	812,124	969,859	28,117	9,906
A6	Whole leaf	Paired-end	50,793,009	39,024,792	89,817,801	2,584,254	4,184,026	6,768,280	78,619	42,621
K1	Whole leaf	Single-end	89,271,083	79,327,402	168,598,485	845,233	2,156,500	3,001,733	42,583	13,653
Art	Epidermal peel	Paired-end	13,366,505	9,982,865	23,349,370	6,130,374	1,969,502	8,099,876	106,326	49,392
Aby	Epidermal peel	Paired-end	9,859,811	10,671,384	20,531,195	1,570,378	1,159,911	2,730,289	68,318	24,353
B103	Epidermal peel	Paired-end	9,848,084	9,967,041	19,815,125	2,470,347	1,488,319	3,958,666	71,324	26,809
Will	Epidermal peel	Paired-end	12,018,656	9,907,614	21,926,270	1,914,323	3,204,741	5,119,064	85,497	37,039
OU14	Epidermal peel	Paired-end	10,515,803	10,744,043	21,259,846	4,070,952	4,520,591	8,591,543	105,147	50,154
RACE1	Epidermal peel	Paired-end	10,588,505	10,976,275	21,564,780	2,936,580	5,693,300	8,629,880	179,086	89,653

Leaves of the barley cultivar Pallas were inoculated with the different *Bgh* isolates and harvested 16 and 48 h after inoculation. For the first set of samples, RNA was isolated from whole leaves, whereas in the later samples RNA was isolated from epidermal peels to enrich for fungal RNA. Samples were subjected to Illumina paired-end or single-end sequencing. For single-end data, each fragment is represented by one read (fragments = reads), whereas for paired-end data, each fragment is represented by a pair of reads. RNA-sequencing statistics in this table and further expression analyses were based on the count of aligned fragment (i.e., for paired-end data each mapped read-pair is counted once, independent of whether one or both reads in the pair were mapped). RNA-sequencing reads were aligned to the *Bgh* isolate DH14 reference genome (www.blugen.org), and all reads that aligned with MAPQ $\geq$ 10 were retained for further analysis.

*The depicted total SNP numbers were derived from the RNA-seq alignment to the DH14 genome by running the samtools mpileup function individually for each isolate.

†To remove potentially unreliable SNP calls, the individual SNP sets were subsequently filtered, thereby excluding all calls for which at least one of the following criteria was met: (*i*) sequencing coverage < 3 reads; (*ii*) alternate allele supported by <50% of the mapped reads; (*iii*) SNP calling quality score < 50; (*iv*) genotype quality score < 10; or (*v*) significant strand ($P > 1e^{-10}$) or tail distance ($P > 1e^{-5}$) bias was detected.

Table S3. List of primers used in this study

Gene	Purpose	Forward primer	Reverse primer
AVR_{a1}	Cloning into pENTR	5′-caccATGCGAACGTGGCAATGCCCAAGCGGTG-3′	CTAGGTGCATTCTTCAATGAATTTTCGG
AVR_{a1}-V1	Cloning into pENTR	caccATGCGAACGTGGCAATGCCGAAGCGGTG	CTAGGTGCATTCTTCAATGAATTTTCGG
AVR_{a1}-V2	Cloning into pENTR	caccATGCAAACTTGGCATTGCAAAAGCGGTG	CTAGGTGCATTCTTCAATGAATTTTCGG
AVR_{a13}-1	Cloning into pENTR	caccATGGCTGGCGATGGTTATATTACCCTTGG-TATGGGG	CTATTCAGGGCTTGAAACCATACAGG
AVR_{a13}-3	Cloning into pENTR	caccATGGCTGGCGATGGTTATATTACCCTTGG-TATGGGG	CTATTCAGGGCTTGAAACCATACAGG
AVR_{a13}-V1	Cloning into pENTR	caccATGGCTGGCGATGGTTATATTACCCTTGG-TATGGGG	TTAGACTATTGGAAATATCCGTGTTACC
AVR_{A13}-V2	Cloning into pENTR	caccATGGCTGGCGATGGTTATATTACCCTTGG-TATGGGG	TTATAGTGTCGCCCGCACTTCATATCTCGCACC
AVR_{A1}-FLAG	Site-directed mutagenesis (template *AVR_{A1}*)	/PHOS/gagtcaggagcaaagcaaggagagaag-ggtGACT ACAAGGATG ACGATGACAAGggaggtggatc-atgaAA GGGTGGGCGCGCCGACCCAGCTTTCTTGTACA-AAGTTGGCATTATA	/PHOS/GGTGCATTCTTCAATGAATTTTCGGT-TATTTCGATAGCCCTGTTGGTATACTACTG-CCACTCGTTTATTTGAAGTAAAGACAGCAA-AAGTTGTTGCGCTAGATGACGAAGGATGCA-CATCCAA TAC C
AVR_{a1}-V1-FLAG	Site-directed mutagenesis (template *AVR_{A1}-V1*)	/PHOS/gagtcaggagcaaagcaaggagagaagg-gtGACTACAAGGATG ACGATGACAAGggaggt-ggatcatgaAAGGGTGGGCGCGCCGACCCAGCT-TTCTTGTACAAAGTTGGCATTATA	/PHOS/GGTGCATTCTTCAATGAATTTTCGGT-TATTTCGATAGCCCTGTTGGTATACTACTG-CCACTCGTTTATTTGAAGTAAAGACAGCAA-AAGTTGTTGCGCTAGATGACGAAGGATGCA-CATCCAGTACC
AVR_{a1}-V2-FLAG	Site-directed mutagenesis (template *AVR_{A1}-FLAG*)	/PHOS/ccatgCAAACTTGGCATTGCAAAAGCGGT-GACATAATTTATG	/PHOS/GTGTTCAAAGGAATTCATATTTGTAT-GTGAATAAACATCTTCTT
FLAG-AVR_{a13}-1	Cloning into pENTR	caccatgGACTACAAGGATGACGATGACAAGagcG-CTGGCGATGGTTATATTac	TAGCTATTCAGGGCTTGAAACCATACAGGTCT-CATATCTCGCAC
FLAG-AVR_{a13}-3	Cloning into pENTR	caccatgGACTACAAGGATGACGATGACAAGagcG-CTGGCGATGGTTATATTac	TAGCTATTCAGGGCTTGAAACCATACAGGTCT-CATATCTCGCAC
FLAG-AVR_{a13}-V1	Cloning into pENTR	caccatgGACTACAAGGATGACGATGACAAGagcG-CTGGCGATGGTTATATTac	TTAGACTATTGGAAATATCCGTGTTACCGAGC-CGTTTATTTC
FLAG-AVR_{a13}-V2	Cloning into pENTR	caccatgGACTACAAGGATGACGATGACAAGagcG-CTGGCGATGGTTATATTac	TTATAGTGTCGCCCGCACTTCATATCTCGCACC
AtUbq10pro-intron	Cloning of the *Arabidopsis* Ubiquitin 10 promoter including the first intron into pDONRG-P4P1R	ggggacaactttgtatagaaaagttggaGGTCATT-GGACTGAACACGAG	ggggactgctttttttgtacaaacttgtCTGTT-AATCAGAAAAACTCAGA
AVR_{a1}	Genotyping transgenic plants	GAAGAAGATGTTTATTCACATAC	CAATACCTTGTAAACGACACCGC
AVR_{a1}	Genotyping transgenic plants	AGTTTGTGCGATCGAATTTGT	CAATACCTTGTAAACGACACCGC
Mla1	Genotyping transgenic plants	CACCATGAAAAGAAATGAAGATCATCAA	CCAAGATTACATCGTGACAG
Mla1	Genotyping transgenic plants	GCGAGGGTGGATAAAGAGAG	TCGAAAGTCAACCGTACAGC

Other Supporting Information Files

Dataset S1 (XLS)